Optical Resolution of 3-Hydroxycarboxylic Acids *via* Diastereomeric Salt Formation

（ジアステレオマー塩法による **3**-ヒドロキシカルボン酸類の光学分割）

A thesis submitted for the degree of

Doctor of Engineering (D.Eng.)

Chandrasekaran Srinivas

19DS055

Graduate School of Science and Engineering

Saitama University, Japan

2023

Table of Contents

Abbreviations

MA	Mandelic acid
TA	Tropic acid
ADPE	2-amino-1,2-diphenylethanol
2-Cl-TA	2-chlorotropic acid
3-Cl-TA	3-chlorotropic acid
4-Cl-TA	4-chlorotropic acid
2-Br-TA	2-bromotropic acid
2-F-TA	2-fluorotropic acid
TMSCHN$_2$	Trimethylsilyldiazomethane
THF	Tetrahydrofuran
DMSO	Dimethyl sulfoxide
AcOEt	Ethyl acetate
Rac	Racemic
Ee	Enantiomeric excess
Eff	Efficiency
HPLC	High-performance liquid chromatography
NMR	Nuclear magnetic resonance
XRD	X-ray diffraction spectroscopy
FT-IR	Fourier-transform infrared spectroscopy
MALDI-TOF-MS	Matrix-assisted laser desorption/ionization - Time of flight mass spectrometry
Ppm	Parts per million

Abstract

In this Ph.D. thesis, I investigate optical resolution of 3-hydroxycarboxylic acids *via* diastereomeric salt formation. The purpose of this study is to develop a facile, and cost-effective method for the optical resolution of 3-hydroxycarboxylic acids *via* diastereomeric salt formation.

This thesis contains four chapters. **Chapter 1** describes chirality, enantiomers, designation of enantiomers (absolute configuration and optical rotation), characteristics and applications of enantiomers, diastereomers, methods of obtaining pure enantiomers (asymmetric synthesis and optical resolution), methods of optical resolution, optical resolution via diastereomeric salt formation, solvent-induced chirality switching resolution, and 3-hydroxycarboxylic acids.

Chapter 2 demonstrates the optical resolution of chlorine-substituted TAs by diastereomeric salt formation with (1*R*,2*S*)-(−)-ADPE. Efficient solvent-induced chirality switching was observed in the case of *rac*-2-Cl-TA. The recrystallization of the diastereomeric salts of *rac*-2-Cl-TA from branched alcohols such as *i*-PrOH and *s*-BuOH afforded (*R*)-2-Cl-TA, whereas (*S*)-2-Cl-TA was obtained from linear alcohols such as MeOH, EtOH, and *n*-PrOH. The chirality switching mechanism was elucidated from the crystal structures of the diastereomeric salts, which revealed that the incorporation of solvent in the (*S*)-2-Cl-TA salt crystals played a key role in chirality switching by reinforcing the supramolecular structure of

the salt. However, no chirality switching was achieved for *rac*-3-Cl-TA and 4-Cl-TA. The position of the chlorine substituent plays an important role in the solvent-induced chirality switching effect.

Chapter 3 represents the optical resolution of a 3-hydroxycarboxylic acid with a more flexible substituent via diastereomeric salt formation using cinchonidine. The resolution of racemic 3-hydroxy-5-phenylpentanoic acid (*rac*-**3**) with cinchonidine afforded (*R*)-salt. In particular, highly efficient optical resolution was afforded by crystallization in toluene. Moreover, the resolution of *rac*-**3** with cinchonidine afforded very good results than the resolution of *rac*-**3** with (−)-ADPE. Crystallographic analysis revealed that hydrogen bonding and CH/π interactions played a crucial role in chiral recognition by reinforcing the supramolecular structure of diastereomeric salt.

Chapter 4 summarizes the conclusion of the Ph.D. thesis as well as the future prospects. The solvent-induced chirality switching resolution will provide an unsophisticated technique for accessing both enantiomers of 2-F-TA, and 2-Br-TA without changing the resolving agent. The optical resolution via diastereomeric salt formation method will provide a guiding concept for us to access the enantiomers of 3-hydroxycarboxylic acids with a more flexible substituent like 3-hydroxy-6-phenylhexanoic acid, and 3-hydroxy-7-phenylheptanoic acid with simple and economical operations.

CHAPTER 1

General Introduction

1.1 Chirality:

Chirality is a geometric property of an object which is non-superimposable on its mirror image by any combination of rotations, translations, and some conformational changes. The objects that cannot be brought into congruence with their mirror images are chial objects. Such objects are devoid of symmetry elements which include reflection: mirror planes, inversion centers, or improper rotational axes. The terms chiral and chirality were coined by W. H. Thompson (Lord Kelvin) and are derived from *cheir*, the Greek word for a hand, indeed one of the most familiar chiral objects.[1] In Fig. 1.a, the left hand and the right hand cannot be superimposed on each other and hence they are chiral whereas in Fig. 1.b, the two conical flasks can be superimposed on each other and they are regarded as achiral.
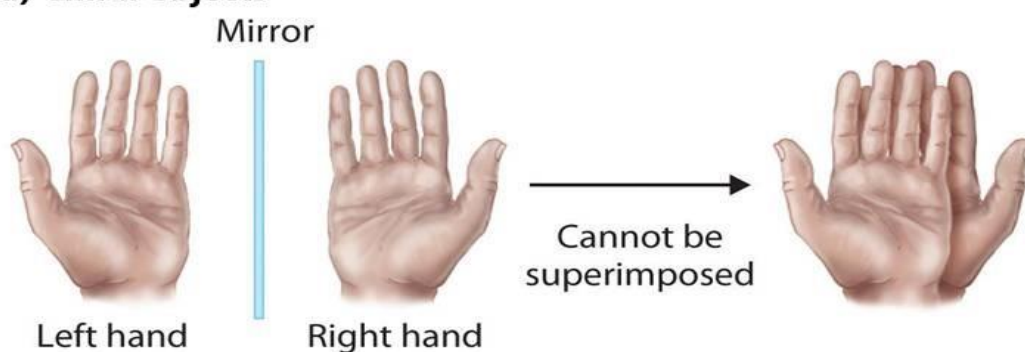
Fig. 1. Chiral and achiral objects.

1.2 Enantiomers:

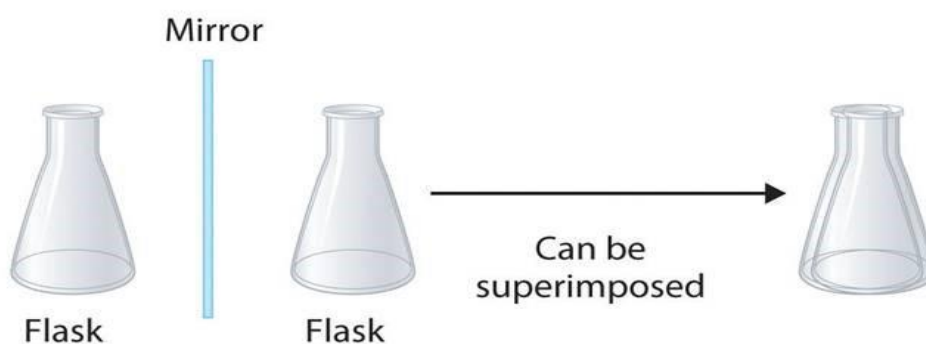The two non-superimposable mirror image forms of chiral molecules are called enantiomers. The term enantiomer was derived from ancient Greek, *enantios* (opposite) and *meros* (part). Enantiomers are also known as optical isomers. They are most commonly formed when a carbon atom (asymmetric carbon atom or stereogenic carbon or also called chiral center) contains four different substituents (Fig. 2). A single chiral atom or similar structural feature in a compound causes that compound to have two possible structures which are non-superposable, each a mirror image of the other. Each member of the pair is termed an enantiomorph (*enantio* = opposite; *morph* = form); the structural property is termed as enantiomerism. The presence of multiple chiral features in a given compound increases the number of geometric forms possible, though there may still be some perfect-mirror-image pairs. Enantioselectivity is the preference for the formation of one enantiomer over the other. A sample of a chemical is considered *enantiopure* (also termed enantiomerically pure) when it has, within the limits of detection, molecules of only one chirality. An equimolar mixture (50/50) of the two enantiomers of a chiral compound is called a racemate, designated as *rac.* or (±).[2]
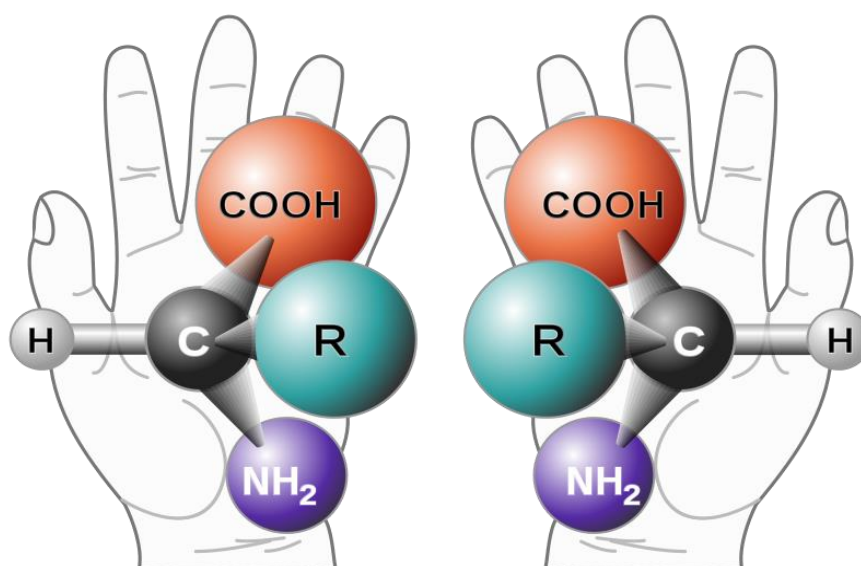

Fig. 2. Two enantiomers of a generic amino acid that is chiral.

Designation of enantiomers:

Absolute configuration (*R/S* system):

Absolute configuration refers to the spatial arrangement of atoms within a chiral molecular entity (or group) and its resultant stereochemical description. Absolute configuration is typically relevant in organic molecules, where carbon is bonded to four different substituents. This type of construction creates two possible enantiomers. Absolute configuration uses a set of rules to describe the relative positions of each bond around the chiral center. The most common labeling method uses the descriptors *R* or *S* is based on the Cahn–Ingold–Prelog priority rules. R and S refer to Rectus and Sinister, which are Latin for right and left, respectively.

Absolute configurations for a chiral molecule (in pure form) are most often obtained by X-ray crystallography, although with some important limitations. All enantiomerically pure chiral molecules crystallize in one of the 65 Sohncke groups (chiral space groups). Alternative techniques include optical rotatory dispersion, vibrational circular dichroism, the use of chiral shift reagents in proton NMR and Coulomb explosion imaging.

The *R / S* system is an important nomenclature system for denoting enantiomers. This approach labels each chiral center *R* or *S* according to a system by which its substituents are assigned a *priority*, according to the Cahn–Ingold–Prelog priority (CIP) rules , based on atomic number (when comparing the atomic number of the atoms directly attached to the stereocenter, the group having the atom of higher atomic number receives higher priority). When the center is oriented and the lowest-priority substituent of the four is pointed away

4

from the viewer, the viewer will then see two possibilities: if the priority of the remaining three substituents decreases in clockwise direction, it is labeled *R* (for *Rectus*, Latin for right); if it decreases in counterclockwise direction, it is *S* (for *Sinister*, Latin for left). (*R*) or (*S*) is written in italics and parentheses (Fig. 3).
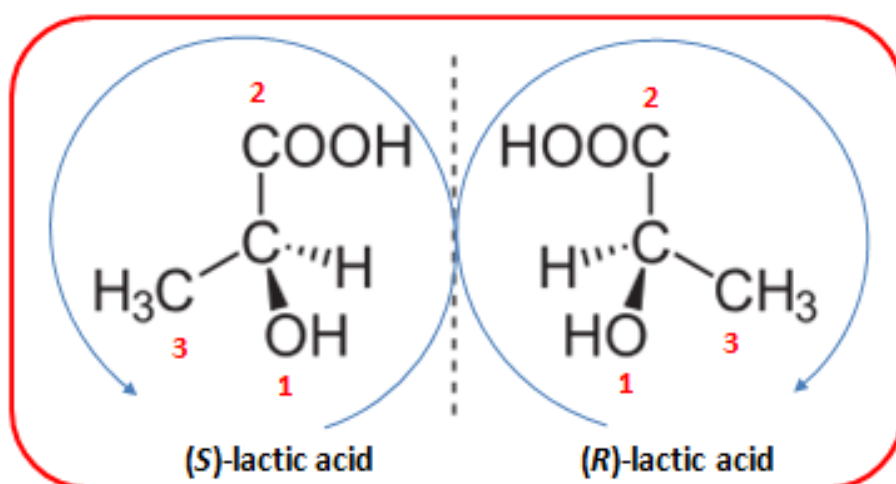
Fig. 3. (*S*)-lactic acid (left) and (*R*)-lactic acid (right).

Optical rotation (+/− system):

Optical rotation, also known as polarization rotation or circular birefringence, is the rotation of the orientation of the plane of polarization about the optical axis of linearly polarized light as it travels through certain materials. Circular birefringence and circular dichroism are the manifestations of optical activity. Optical activity occurs only in chiral materials, those lacking microscopic mirror symmetry. Unlike other sources of birefringence which alter a beam's state of polarization, optical activity can be observed in fluids. This can include gases or solutions of chiral molecules such as sugars, molecules with helical secondary structure such as some proteins, and also chiral liquid crystals. It can also

5

be observed in chiral solids such as certain crystals with a rotation between adjacent crystal planes (such as quartz) or metamaterials.

Optical activity is measured using a polarized source and polarimeter (Fig. 4). This is a tool particularly used in the sugar industry to measure the sugar concentration of syrup, and generally in chemistry to measure the concentration or enantiomeric ratio of chiral molecules in solution. When looking at the source of light, the rotation of the plane of polarization may be either clockwise (represented by "(+)"), or counter-clockwise, (represented by "(−)"), depending on which stereoisomer is dominant. For a given substance, the angle by which the polarization of light of a specified wavelength is rotated is proportional to the path length through the material and (for a solution) proportional to its concentration.
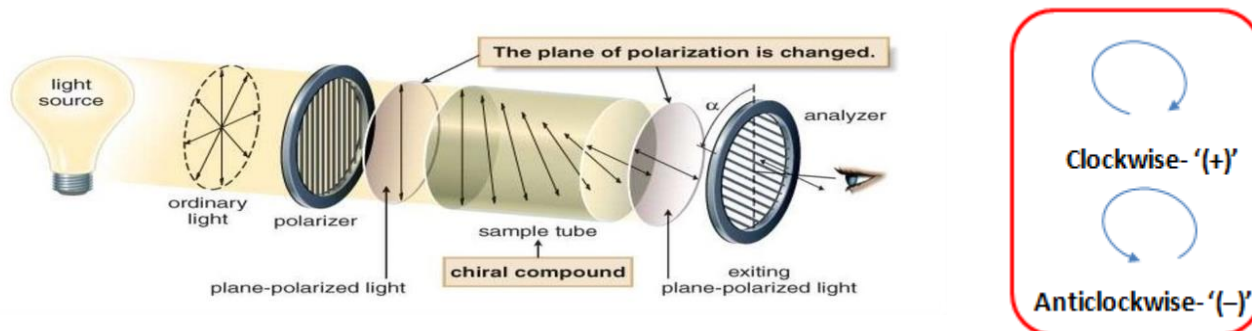
Fig. 4. Optical activity in chiral compounds.

(cited from the URL: https://physicsopenlab.org/2019/08/20/optical-activity-chirality/)

Characteristics of enantiomers:

Enantiomers have the same chemical formula, the same physical and chemical properties (solubility, boiling point, melting point, reactivity etc,.). They differ in their optical activity and spatial arrangement.

Enantiomer members often have different chemical reactions with other enantiomer substances. Since many biological molecules are enantiomers, there is sometimes a marked difference in the effects of two enantiomers on biological organisms. Especially in the case of drugs, getting an appropriate enantiomer is necessary.

Often only one of a drug's enantiomers is responsible for the desired physiological effects (referred to as eutomer), while the other enantiomer is less active, inactive, or sometimes even productive of adverse effects (referred to as distomer). For example, in the case of penicillamine, the (S)-enantiomer (eutomer) is antiarthritic while the (R)-enantiomer (distomer) is extremely toxic (Fig. 5).
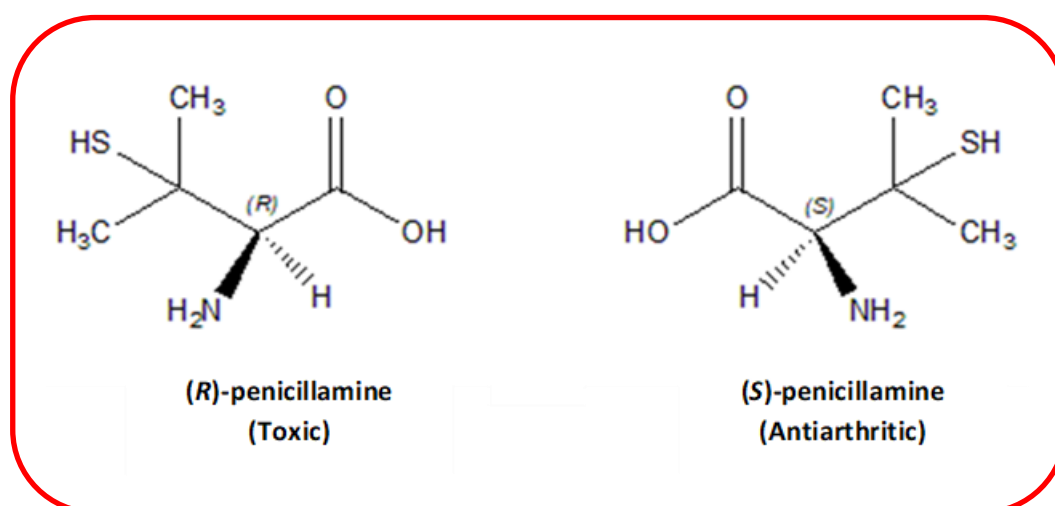
Fig. 5. Different biological activities of penicillamine enantiomers.

Owing to this discovery, drugs composed of only one enantiomer ("enantiopure") can be developed to make the drug work better and sometimes eliminate some side effects. An example is eszopiclone (Lunesta), which is the (*S*)-enantiomer of an older racemic drug called zopiclone (Fig. 6). This is a typical example of a chiral switch (chiral drugs that are already approved as racemates, but that have been re-developed as single enantiomers). The (*S*)-enantiomer is responsible for all the desired effects, while the (*R*)-enantiomer seems to be inactive, so the dose of eszopiclone is half that of zopiclone.[3-5]
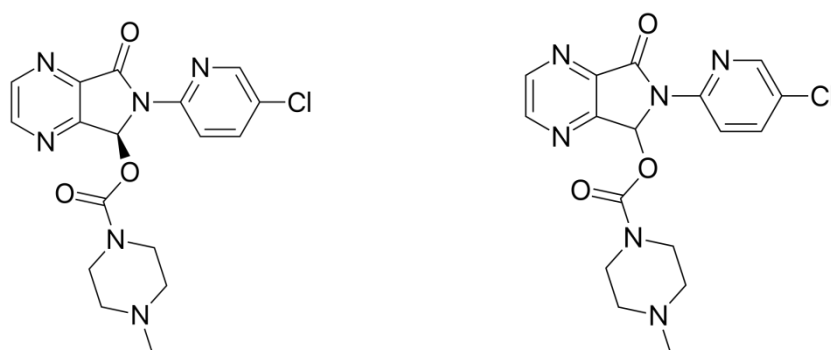
Fig. 6. Chemical structures of Eszopiclone (left) and Zopiclone (right).

Applications of enantiomers:

Enantiopure chiral molecules are essential in pharmaceuticals, agrochemicals, food supplements, optoelectronic devices, cosmetics, fragrances, flavors, and additives to modify polymer properties. In particular, about more than half of the drugs currently in use are chiral compounds. This reveals the practical significance of chirality and methods of obtaining enantiopure compounds. Moreover, tremendous research is focussed on novel applications of chiral compounds in industries.[6,7]

1.3 Diastereomers:

Diastereomers are molecules with multiple chiral centers, which have the same atoms and bonds but different stereochemistry in at least one, but not all, of their chiral centers (Fig. 7). These stereoisomers are non-superimposable; not mirror images of each other. When two diastereoisomers differ from each other at only one stereocenter they are epimers. Each stereocenter gives rise to two different configurations and thus typically increases the number of stereoisomers by a factor of two. Diastereomers are different from enantiomers; the latter are pairs of stereoisomers that differ in all stereocenters and are therefore mirror images of one another. Enantiomers of a compound with more than one stereocenter are also diastereomers of the other stereoisomers of that compound that are not their mirror image (that is, excluding the opposing enantiomer).

Unlike enantiomers, diastereomers have different physical and chemical properties. This knowledge is harnessed in chiral synthesis to separate a mixture of enantiomers. This is the principle behind chiral resolution. After preparing the diastereomers, the diastereomers are separated by chromatography or recrystallization.[8] Diastereoselectivity is the preference for the formation of one or more than one diastereomer over the other in an organic reaction.
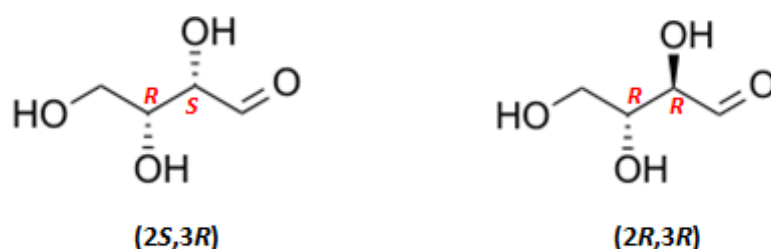
Fig. 7. Diastereomers of 2,3,4-trihydroxybutanal.

1.4 Methods of obtaining pure enantiomers:

Mainly, there are two important approaches to obtain pure enantiomers (Fig. 8). One approach is "Synthesis" and the other one is "Separation". In synthesis approach, "Asymmetric synthesis" is employed to obtain pure enantiomers whereas in separation approach, pure enantiomers are obtained by "Optical resolution".[9] In this research work, we have focussed on optical resolution.
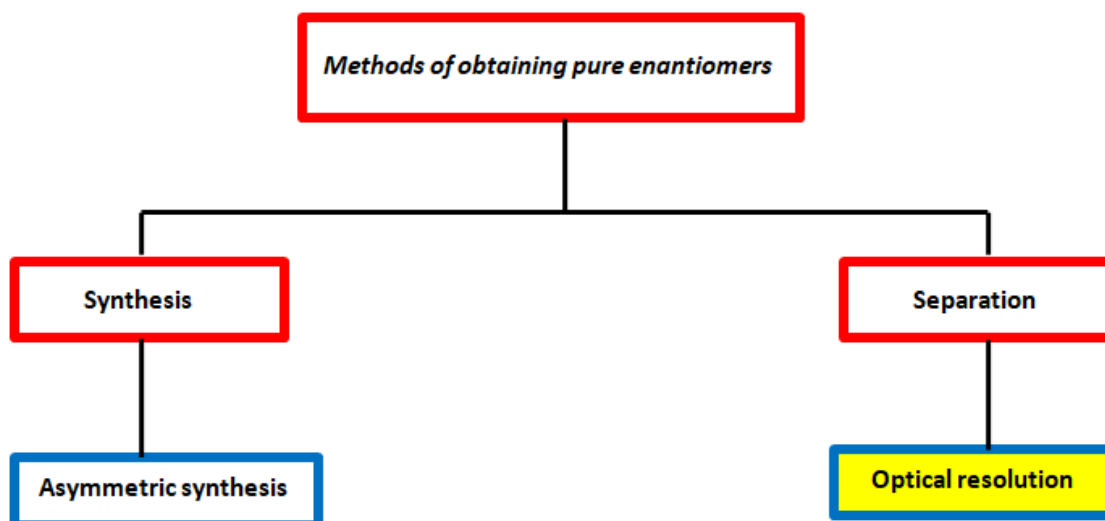
Fig. 8. Methods of obtaining pure enantiomers.

Asymmetric synthesis:

Enantioselective synthesis, also called asymmetric synthesis, is a form of chemical synthesis. It is defined by IUPAC as: a chemical reaction (or reaction sequence) in which one or more new elements of chirality are formed in a substrate molecule and which produces the stereoisomeric (enantiomeric or diastereoisomeric) products in unequal amounts. In

simple terms, it is the selective synthesis of one enantiomeric form of a desired optically active molecule. Asymmetric synthesis is a key process in modern chemistry and is particularly important in the field of pharmaceuticals, as the different enantiomers of a molecule often have different biological activity.[10-13]

Optical resolution:

Optical resolution is a process for the separation of racemates into their enantiomers (Fig. 9). It is also known as chiral resolution, or enantiomeric resolution. It is an important tool in the production of optically active compounds, including drugs. Moreover, it is simple and cost-efficient than asymmetric synthesis for the production of highly pure compounds on an industrial scale.
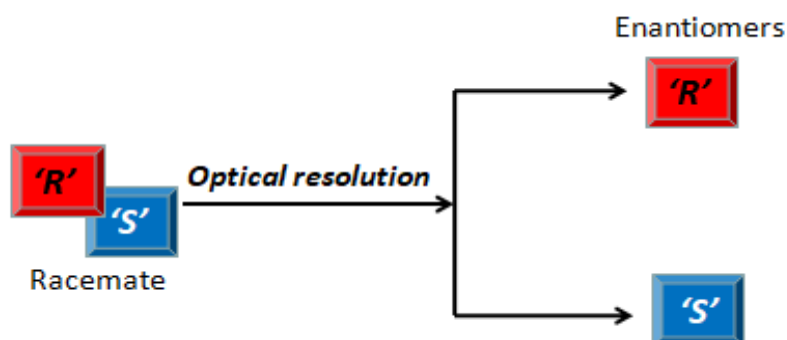
Fig. 9. Optical resolution.

Resolution may serve several purposes:

(i) Structural studies: Pasteur's resolution experiments (1853) paved the way for the discovery of the tetrahedral orientation of the valencies of carbon (van't Hoff and Le Bel, 1874). Resolvability of compounds such as $R^1R^2R^3R^4N^+$ type ammonium salts and $R^1R^2R^3P$ type phosphines provided information about the configurational stability of such compounds.

Racemization rates of atropisomers (atropisomers are stereoisomers that result from a hindrance of bond rotation about single bonds due to steric strain, making the isolation of the individual isomers possible) permits a rough estimation of the bulk of substituents in the *ortho* position to the aryl–aryl bond.

(ii) Mechanistic studies: optically active compounds are powerful tools in the elucidation of the stereochemistry of reactions, especially in biochemistry. For example, the inversion of configuration in S_N2 reactions was recognized by comparing the rate of racemization and isotope exchange of 2-iodooctane. [14]

(iii) Study of the biological activity of the individual enantiomers of chiral compounds.

(iv) Separation of active and inactive (possibly harmful) enantiomers of chiral commercial products, foremost of drugs and pesticides. Nowadays the chances for registration of a new chiral drug in its racemic form are slim. [15]

1.5 Methods of optical resolution:

Since the first separation of enantiomers by Louis Pasteur in 1848, a continuous search for new and efficient resolution procedures can be observed. There are various optical resolution methods as shown in Fig. 10. [16]

In this research work, we have focussed on optical resolution *via* diastereomeric salt formation owing to its simplicity and cost-efficiency.
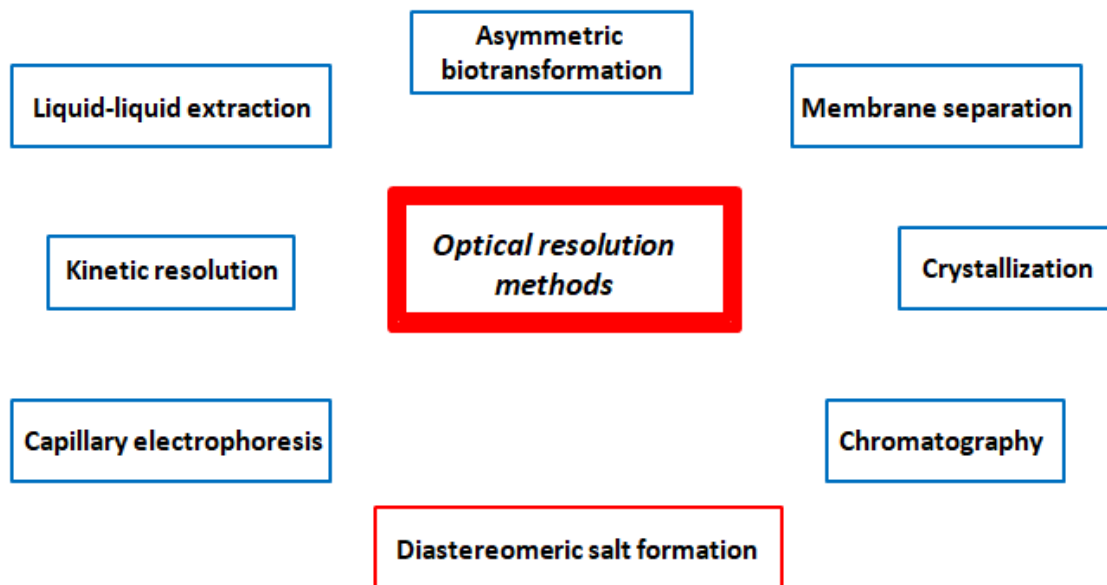
Fig. 10. Methods of optical resolution.

Optical resolution via diastereomeric salt formation:

The optical resolution of racemates via diastereomeric salt formation (Fig. 11) is a widely employed method for obtaining optically pure acidic and basic compounds on an industrial scale. This method is extensively used for acids and bases owing to their ability to form salts. In this method, when a target racemate is combined with an optically active resolving agent, a pair of diastereomeric salts are formed (When the racemate is an acid, the resolving agent would be an optically active base and when the racemate is a base, the resolving agent would be an optically active acid). The diastereomeric salts differ in physical properties like solubility and therefore they can be separated by crystallization. By means of crystallization, the less-soluble diastereomeric salt preferentially crystallizes out and the

more-soluble diasteromeric salt remains in the solution. From the less-soluble diasteromeric salt, we could able to obtain the enantiomer by decomposition (removal of resolving agent). In addition, the optical purity and yield of the diastereomeric salts were dependent on the solvent employed for crystallization.
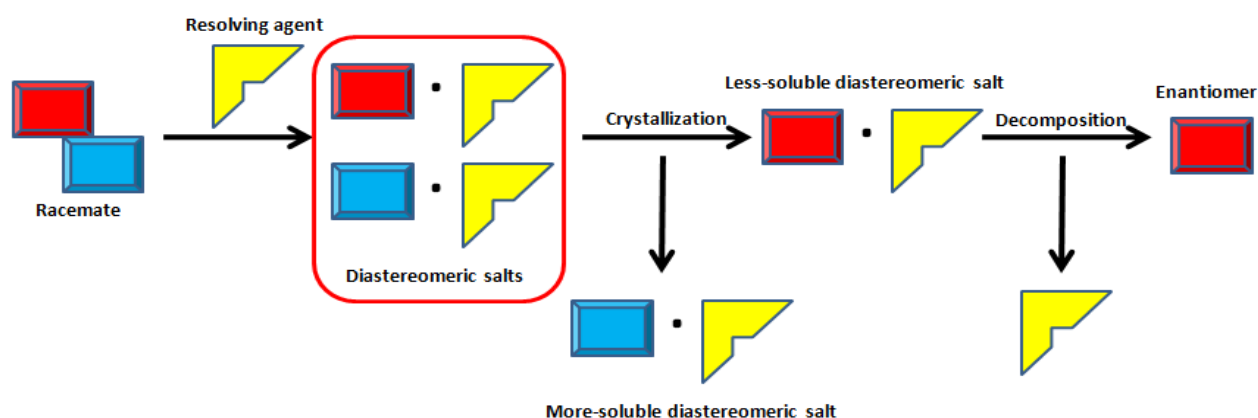
Fig. 11. Optical resolution via diastereomeric salt formation.

This method provides multifaceted advantages, such as simplicity, cost efficiency, recyclability of resolving agents, and repeated crystallization to enhance the optical purity of the less-soluble diastereomeric salt (Fig. 12), that render it an attractive prospect for the pharmaceutical industry. [17,18]
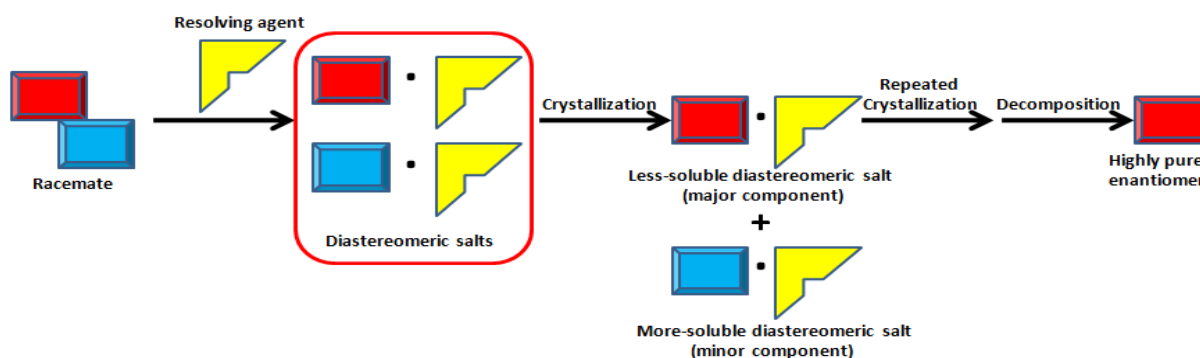
Fig. 12. Repeated crystallization to enhance the optical purity of
the less-soluble diastereomeric salt.

In Fig. 12, when a racemate is combined with an optically active resolving agent, a pair of diastereomeric salts are formed. By crystallization, the less-soluble diastereomeric salt preferentially crystallizes out. But this less-soluble diastereomeric salt (major component) is not pure in almost all cases. It contains some small amounts of the more-soluble diastereomeric salt (minor component). Therefore, by means of repeated crystallization, the optical purity of the less-soluble diastereomeric salt could be enhanced and finally, we could able to obtain the pure enantiomer after the removal of resolving agent by decomposition.

Although this method has several advantages, there are also some drawbacks attributed with this method. It is still difficult to strategically find an appropriate resolving agent. This limits the versatility of this technique as even an infinitesimal structural modification can contribute to an unanticipated molecular packing in the salt crystal.[19-23] Another drawback of this method is that the difficulty of purifying more-soluble diastereomeric salts to obtain the other enantiomer, which allows intricate operations such as decomposition of the salt followed by its reformation with another resolving agent (Fig. 13).[24]

The dielectric constant of the crystallization solvent can also influence the stereochemistry of less-soluble diastereomeric salts in some cases.[25-28] Therefore the crystallization solvent plays an important role in optical resolution.
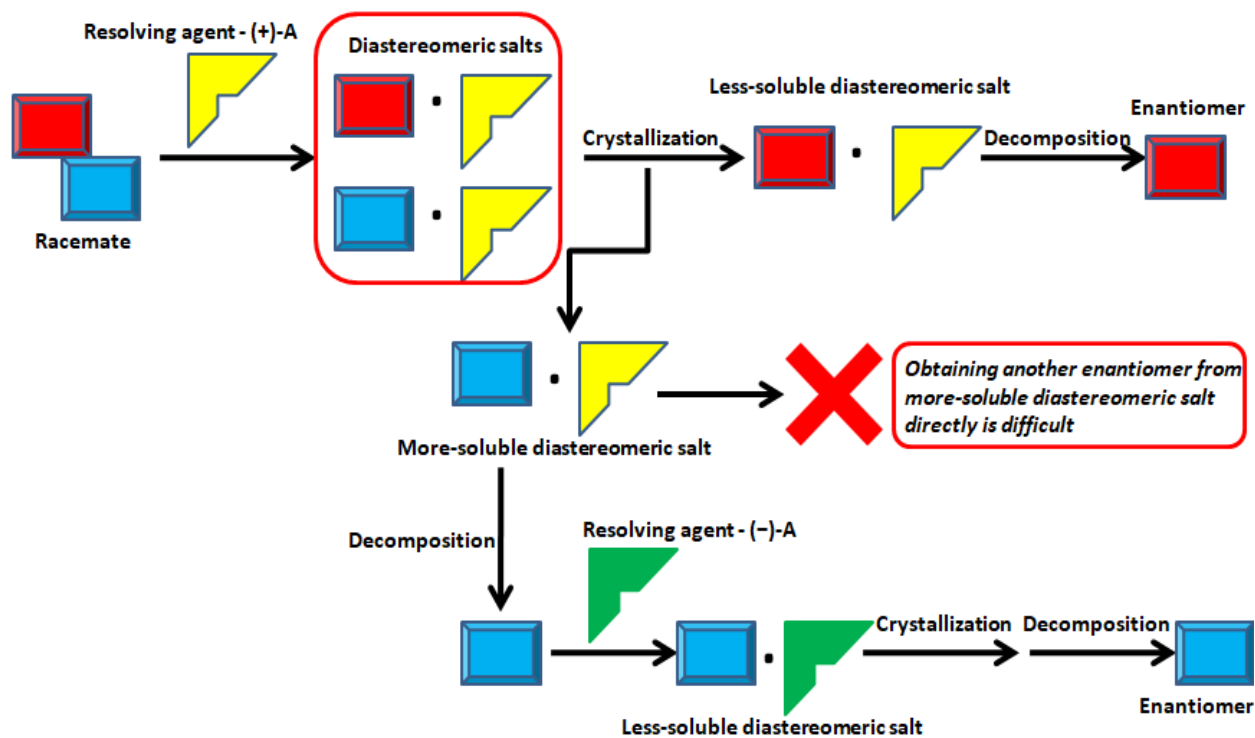
Fig. 13. Purification of more-soluble diastereomeric salts to obtain the other enantiomer, allows intricate operations.

Solvent-induced chirality switching resolution:

In our laboratory, we have developed a special technique called *"Solvent-induced chirality switching resolution"*, where the change in crystallization solvent changes the stereochemistry of the less-soluble diastereomeric salt (Fig. 14). This method enables access to both the enantiomers simultaneously without changing the resolving agent. The solvent inclusion plays an important role in molecular packing of the crystal resulting in efficient optical resolution.[29-31]

Fig. 14. Solvent-induced chirality switching resolution.

In Fig. 14, when a racemate is combined with an optically active resolving agent, a pair of diastereomeric salts are formed. By crystallization from solvent "A", the less-soluble diastereomeric salt preferentially crystallizes out. After the removal of resolving agent by decomposition, we could able to obtain one enantiomer. In order to obtain the another enantiomer, there is no need to change the resolving agent in this method. By simply changing

the crystallization solvent from solvent "A" to solvent "B", we could able to change the stereochemistry of the less-soluble diastereomeric salt and obtain another enantiomer. The solvent inclusion enhances the stability of the crystal by changing its supramolecular structure (*via* various interactions such as hydrogen bonding and CH/π interactions), resulting in efficient optical resolution.

An example of solvent-induced chirality switching resolution:

Chirality switching in racemic MA with (1*R*,2*S*)-(−)-ADPE:

During the optical resolution of *rac*-MA with (1*R*,2*S*)-(−)-ADPE, crystallization from MeOH has afforded the (*S*)-salt of MA, whereas crystallization from *n*-BuOH afforded the (*R*)-salt of MA (Fig. 15). Thus chirality switching was achieved by changing the crystallization solvent.[32]
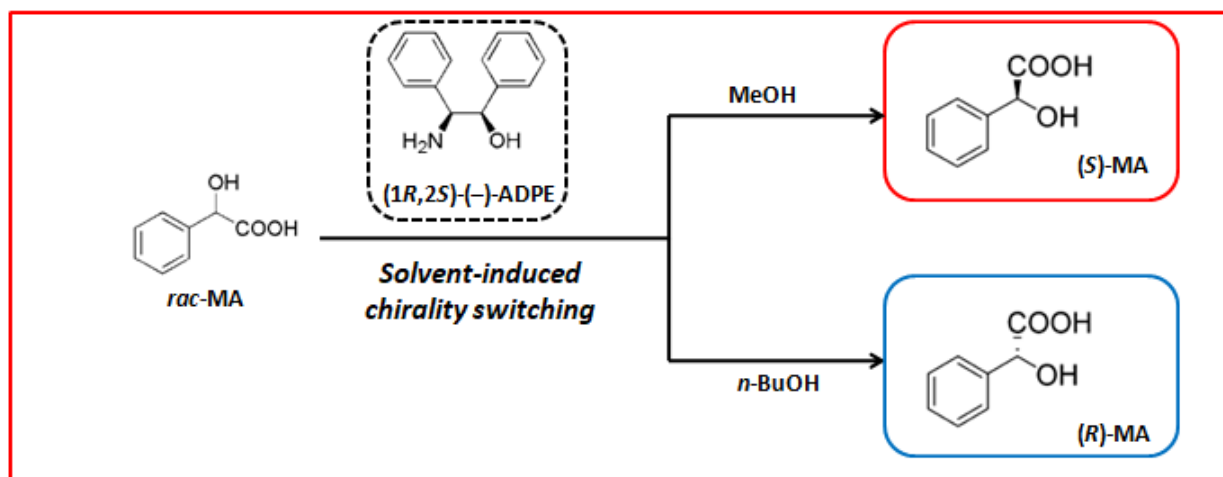
Fig. 15. Solvent-induced chirality switching in *rac*-MA.

1.6 3-Hydroxycarboxylic acids:

Optically pure hydroxycarboxylic acids are important compounds that can be widely employed as chiral precursors because their functional groups can be easily modified. Among the hydroxycarboxylic acids, enantiopure 3-hydroxycarboxylic acids have received considerable attention as they have been proven to be valuable synthons and can be used as starting materials in the synthesis of antibiotics, beta-amino acids, vitamins, flavors, and pheromones.[33-36] They are also vital subunits of polyketide natural products, such as amphotericin B, tylosin, and rosaramicin.[37-40] Moreover, several optically pure 3-hydroxycarboxylic acids exhibit critical biological activities, such as antimicrobial and antiviral potential.[41,42] Examples: optically active 3-hydroxy-3-phenylpropionic acid has been applied to the stereoselective synthesis of chiral drugs such as (*S*)-dapoxetine [43] (Scheme. 1); derivatives of 3-hydroxy-4-phenylbutanoic acid have anti-inflammatory properties; 3-hydroxy-5-phenylpentanoic acid, 3-hydroxy-6-phenylhexanoic acid and 3-hydroxy-7-phenylheptanoic acid have antimicrobial properties (Fig. 16).
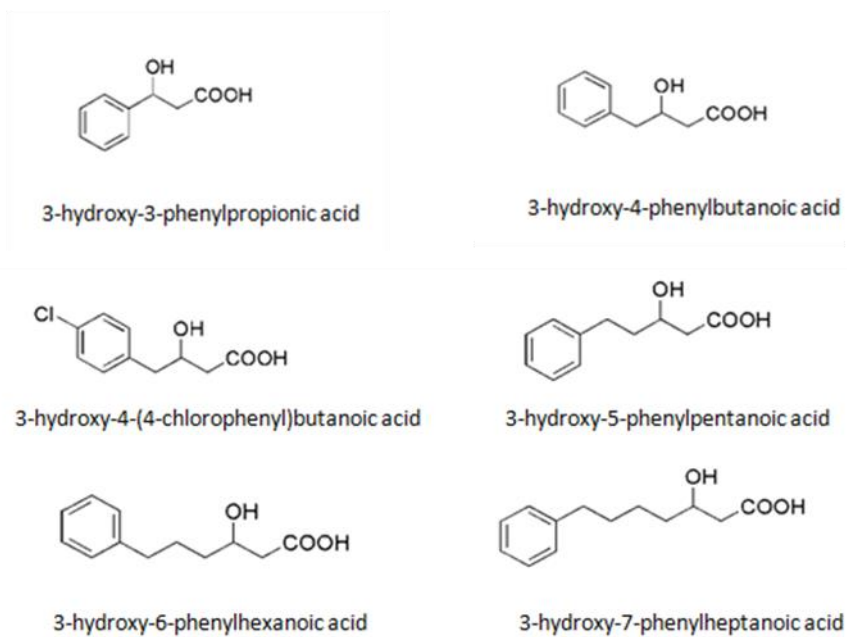
Fig. 16. Chemical structures of 3-hydroxycarboxylic acids.
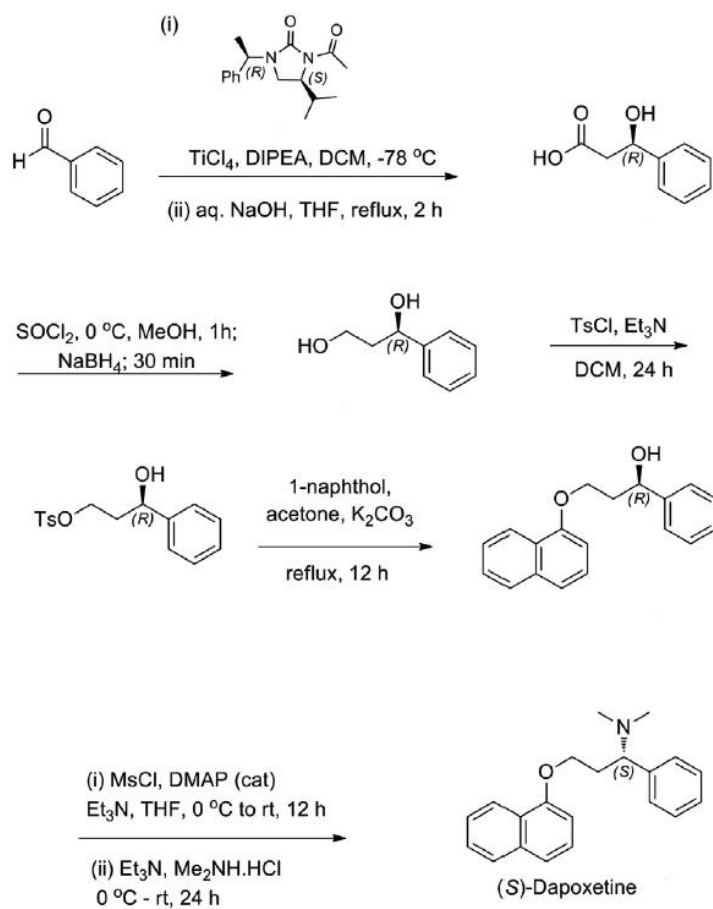
Scheme. 1. Stereoselective synthesis of (*S*)-dapoxetine.

1.7 Aim of this thesis:

In this thesis, I investigate optical resolution of 3-hydroxycarboxylic acids *via* diastereomeric salt formation. The optical resolution of racemates *via* diastereomeric salt formation is one of the most reliable and frequently used methods for obtaining optically pure acidic and basic compounds. On the other hand, enantiopure 3-hydroxycarboxylic acids have received considerable attention as they have been proven to be valuable synthons and can be used as starting materials in the synthesis of antibiotics, beta-amino acids, vitamins, flavors, and pheromones. Hence, the purpose of this study is to develop a facile, and cost-effective method for the optical resolution of 3-hydroxycarboxylic acids *via* diastereomeric salt formation.

1.8 References:

1. Prelog, V. *Science* **1976**, *193*, 17-24.

2. Nguyen, L. A.; He, H.; Pham-Huy, C. *Int. J. Biomed. Sci.* **2006**, *2*, 85-100.

3. McConathy, J.; Owens, M. J. *Prim. Care Companion J. Clin. Psychiatry* **2003**, *5*, 70-73.

4. Aboul-Enein, H. Y.; Wainer, I. W. *The Impact of Stereochemistry on Drug Development and Use*; Wiley: New York, 1997.

5. Gandhi, K.; Shah, U.; Patel, S. *Curr. Drug Discov. Technol.* **2020**, *17*, 565-573.

6. Farina, V.; Reeves, J. T.; Senanayake, C. H.; Song, J. J. *Chem. Rev.* **2006**, *106*, 2734-2793.

7. Wu, G.; Huang, M. *Chem. Rev.* **2006**, *106*, 2596-2616.

8. Jacques, J.; Collet, A.; Wilen, S. H. *Enantiomers, Racemates, and Resolutions*; Wiley & Sons: New York, NY, 1981.

9. Siedlecka, R. *Tetrahedron* **2013**, *69*, 6331-6363.

10. Brown, J. M. *Chem. Soc. Rev.* **1993**, *22*, 25–41.

11. Nogradi, M. *Stereoselective Synthesis: A Practical Approach*; Wiley-VCH: Weinheim, Germany, 1994.

12. Carreira, E. M.; Kvaerno, L. *Classics in Stereoselective Synthesis*; Wiley-VCH: Weinheim, Germany, 2009.

13. Sheldon, R. A. *Chimia* **1996**, *50*, 418–419.

14. Hughes, E. D.; Ingold, C. K. *J. Chem. Soc.* **1940**, 913–1024.

15. Fogassy, E.; Nogradi, M.; Kozma, D.; Egri, G.; Palovics, E.; Kiss, V. *Org. Biomol. Chem.* **2006**, *4*, 3011–3030.

16. Maier, N. M.; Franco, P.; Lindner, W. *J. Chromatogr. A* **2001**, *906*, 3–33.

17. Kozma, D. *Optical Resolutions via Diastereomeric Salt Formation*; CRC: London, 2002.

18. Faigl, F.; Fogassy, E.; Nógrádi, M.; Pálovics, E.; Schindler, J. *Tetrahedron: Asymmetry* **2008**, *19*, 519-536.

19. Karamertzanis, P. G.; Anandamanoharan, P. R.; Fernandes, P.; Cains, P. W.; Vickers, M.; Tocher, D. A.; Florence, A. J.; Price, S. L. *J. Phys. Chem. B* **2007**, *111*, 5326-5336.

20. Bereczki, L.; Bombicz, P.; Balint, J.; Egri, G.; Schindler, J.; Pokol, G.; Fogassy, E.; Marthi, K. *Chirality* **2009**, *21*, 331-338.

21. Palovics, E.; Schindler, J.; Faigl, F.; Fogassy, E. *Tetrahedron: Asymmetry* **2010**, *21*, 2429-2434.

22. He, Q.; Rohani, S.; Zhu, J.; Gomaa, H. *Chirality* **2012**, *24*, 119-128.

23. Wang, P.; Zhang, E.; Niu, J.; Ren, Q.; Zhao, P.; Liu, H. *Tetrahedron: Asymmetry* **2012**, *23*, 1046-1051.

24. Kodama, K.; Hayashi, N.; Yoshida, Y.; Hirose, T. *Tetrahedron* **2016**, *72*, 1387–1394.

25. Sakai, K.; Sakurai, R.; Hirayama, N. *Top. Curr. Chem.* **2007**, *269*, 199–231.

26. Taniguchi, K.; Aruga, M.; Yasutake, M.; Hirose, T. *Org. Biomol. Chem.* **2008**, *6*, 458–463.

27. Sakurai, R.; Sakai, K.; Kodama, K.; Yamaura, M. *Tetrahedron: Asymmetry* **2012**, *23*, 221–224.

28. Schmitt, M.; Schollmeyer, D.; Waldvogel, S. R. *Eur. J. Org. Chem.* **2014**, 1007–1012.

29. Kodama, K.; Kurozumi, N.; Shitara, H.; Hirose, T. *Tetrahedron* **2014**, *70*, 7923–7928.

30. Shitara, H.; Shintani, T.; Kodama, K.; Hirose, T. *J. Org. Chem.* **2013**, *78*, 9309–9316.

31. Kodama, K.; Kawasaki, K.; Yi, M.; Tsukamoto, K.; Shitara, H.; Hirose, T. *Cryst. Growth Des.* **2019**, *19*, 7153–7159.

32. Kodama, K.; Shitara, H.; Hirose, T. *Cryst. Growth Des.* **2014**, *14*, 3549–3556.

33. Thaisrivongs, S.; Pals, D. T.; Kati, W. M.; Turner, S. R.; Thomasco, L. M.; Watt, W. *J. Med. Chem*. **1986**, *29*, 2080.

34. Schostarez, H. J. *J. Org. Chem*. **1988**, *53*, 3628.

35. Oertle, K.; Beyeler, H.; Duthaler, R. O.; Lottenbach, W.; Riediker, M.; Steiner, E. *Helv. Chim. Acta* **1990**, *73*, 353.

36. Seidel, W.; Seebach, D. *Tetrahedron Lett.* **1982**, *23*, 159-162.

37. Masamune, S.; Choy, W.; Petersen, J. S.; Sita, L. R. *Angew. Chem., Int. Ed. Engl.* **1985**, *24*, 1.

38. Nicolaou, K. C.; Chakraborty, T. K.; Ogawa, Y.; Daines, R. A.; Simpkins, N. S.; Furst, G. T. *J. Am. Chem. Soc*. **1988**, *110*, 4660.

39. Tatsuta, K.; Amemiya, Y.; Kanemura, Y.; Takahashi, H.; Kinoshita, M. *Tetrahedron Lett.* **1982**, *23*, 3375.

40. Schlessinger, R. H.; Poss, M. A.; Richardson, S. *J. Am. Chem. Soc.* **1986**, *108*, 3112.

41. Sandoval, A.; Arias-Barrau, E.; Bermejo, F.; Canedo, L.; Naharro, G.; Olivera, E.; Luengo, J. *Appl. Microbiol. Biotechnol.* **2005**, *67*, 97-105.

42. Burke, T. R.; Knight, M.; Chandrasekhar, B. *Tetrahedron Lett.* **1989**, *30*, 519-522.

43. Khatik, G. L.; Sharma, R.; Kumar, V.; Chouhan, M.; Nair, V. A. *Tetrahedron Lett.* **2013**, *54*, 5991–5993.

CHAPTER 2

"*Solvent-Induced Chirality Switching*" in the Enantioseparation of Chlorine-Substituted Tropic Acids *via* Diastereomeric Salt Formation

2.1 Introduction:

The optical resolution of racemates via diastereomeric salt formation is a widely employed method for obtaining optically pure acidic and basic compounds on an industrial scale.[1-4] In this method, a target racemate is combined with an optically active resolving agent and enantioseparation is enabled by crystallization. The less-soluble diastereomeric salt preferentially crystallizes out and the more-soluble diastereomeric salt remains in the solution owing to their different solubilities. The method provides multifaceted advantages, such as simplicity, cost efficiency, recyclability of resolving agents, and repeated crystallization to enhance the optical purity of the less-soluble diastereomeric salt, that render it an attractive prospect for the pharmaceutical industry. However, it is still difficult to strategically find an appropriate resolving agent. This limits the versatility of this technique as even an infinitesimal structural modification can contribute to an unanticipated molecular packing in the salt crystal.[5-9] Another drawback of this method is that the difficulty of purifying more-soluble diastereomeric salts to obtain the other enantiomer, which allows intricate operations such as decomposition of the salt followed by its reformation with another resolving agent.[10] In addition, the optical purity and yield of the diastereomeric salts were dependent on the solvent employed for crystallization. The dielectric constant of the crystallization solvent can also influence the stereochemistry of less-soluble diastereomeric salts in some cases.[11-14]

Optically pure hydroxycarboxylic acids are important compounds that can be widely employed as chiral precursors because their functional groups can be easily modified.

Optically pure TA and its derivatives are important compounds for the production of pharmaceuticals. Among the TA derivatives reported to date, chlorine-substituted TA is important as it can be easily functionalized into other TA derivatives by cross-coupling reactions. Enantiopure chlorine-substituted TA is an important chiral building block of hyoscyamine derivatives.[15,16] It is widely known that (*R*)-hyoscyamine exhibits analgesic activity whereas (*S*)-hyoscyamine is an antagonist of the muscarinic receptor.[17-20] Some enzymatic resolutions of TA have already emerged.[21-24] A few reports of its chemical resolutions have also appeared.[25-28] Previously, we reported solvent-induced chirality switching during the optical resolution of racemic TA using (1*R*,2*S*)-(−)-ADPE. Recrystallization of the diastereomeric salt mixture in EtOH and *i*-PrOH yielded the (*S*)-TA salt. In contrast, the (*R*)-TA salt was deposited in water-enriched alcohol solutions and 1,4-dioxane. Chirality switching was achieved using two different solvents. The solvent alcohols incorporated in the salt crystals of (*S*)-TA played a key role in chirality switching by changing the supramolecular structure of the salt.[29]

Although resolution by solvent-induced chirality switching has been successfully applied to MA[30,31] and its halogen-substituted derivatives,[32] allowing access to both enantiomers in a highly efficient manner, this method has not been applied to halogen-substituted derivatives of TA. The flexible methylene group of TA derivatives makes their resolution difficult when compared to MA derivatives. To expand the scope of resolution by solvent-induced chirality switching, *rac*-2-Cl-TA, *rac*-3-Cl-TA, and *rac*-4-Cl-TA were selected as the target chiral carboxylic acids in this study. Herein, we report the synthesis of the above-mentioned target compounds and demonstrate an efficient solvent-induced chirality

switching effect in the optical resolution of *rac*-2-Cl-TA with (−)-ADPE via diastereomeric salt

formation, which enabled access to both enantiomers simultaneously without changing the

resolving agent. The mechanism was elucidated through analysis of the crystal structures of

the diastereomeric salts prepared from each solvent.
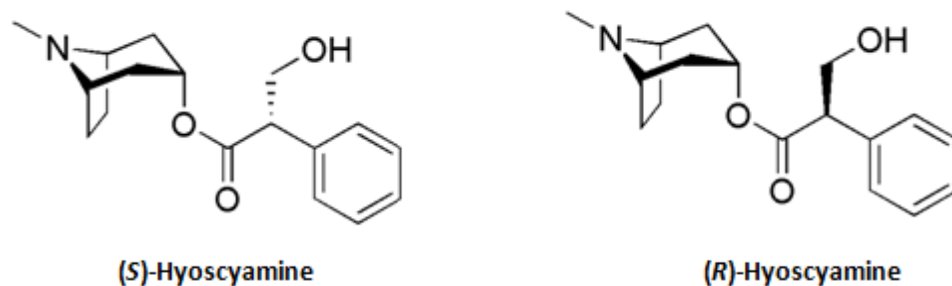
Fig. 1. Enantiomers of hyoscyamine.
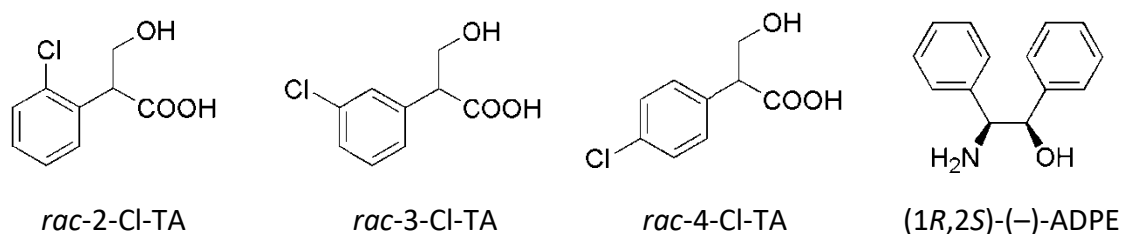
Fig. 2. Structures of *rac*-2-Cl-TA, *rac*-3-Cl-TA, *rac*-4-Cl-TA, and (1*R*,2*S*)-(−)-ADPE.

2.2 Results and Discussion:

Synthesis of Chlorine-substituted TAs:

The chlorine-substituted TAs have been synthesized (Scheme. 1) and utilized for the optical resolution experiments. The detailed experimental procedure for the synthesis of chlorine-substituted TAs has been mentioned in the experimental section.
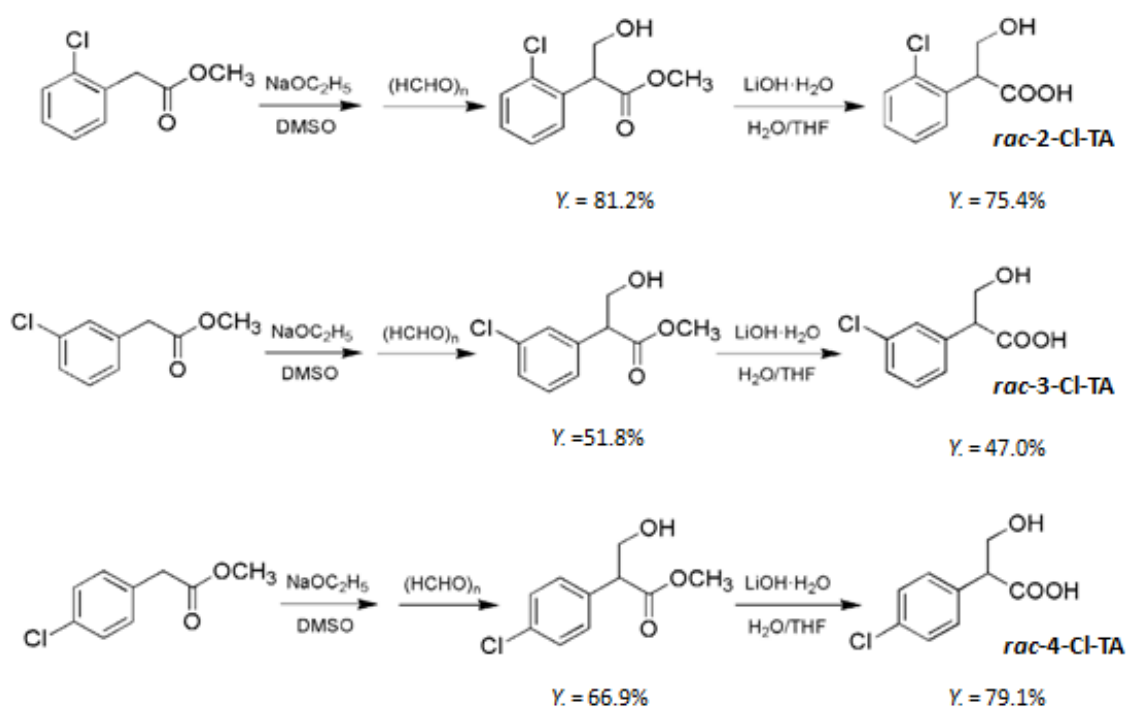
Scheme. 1. Synthesis of Chlorine-substituted TAs.

Optical resolution of *rac*-2-Cl-TA with (1*R*,2*S*)-(−)-ADPE:

The influence of the solvents employed for recrystallization during the optical resolution of *rac*-2-Cl-TA with (−)-ADPE was investigated. The initial diastereomeric salt mixture was prepared by dissolving equimolar quantities of *rac*-2-Cl-TA and (−)-ADPE in

methanol, followed by evaporation. It was then recrystallized from various solvents such as water, alcohols, aqueous ethanol, and cyclic ethers. After the deposited salt crystals were characterized by ^{1}H NMR analysis, a small quantity of salt was utilized to extract 2-Cl-TA. The recovered 2-Cl-TA was converted to its corresponding methyl ester and its enantiopurity was determined by HPLC analysis (Table 1).

Table 1: Optical resolution of *rac*-2-Cl-TA with (–)-ADPE[a]

Entry	Recrystallization solvent (mL)	Ratio of the salt to solvent included[b]	Yield %[c]	Ee %[d]	Eff.[e]
1	H$_2$O (2.5)	Not included	50.6	13 (*R*)	0.07
2	30% EtOH (4)	Not included	99.9	6 (*R*)	0.06
3	50% EtOH (5)	1:0.5	63.2	30 (*S*)	0.19
4	MeOH (1)	1:0.7	20.1	97 (*S*)	0.19
5	EtOH (7)	1:0.9	76.9	87 (*S*)	0.67
6	*n*-PrOH (7)	1:0.3	96.6	23 (*S*)	0.22
7	*i*-PrOH (3.5)	Not included	71.9	31 (*R*)	0.22
8	*s*-BuOH (8.5)	Not included	56.9	30 (*R*)	0.17
9	THF (3)	Not included	30.1	38 (*R*)	0.11
10	1,4-dioxane (7)	Not included	33.6	*rac.*	0
11	Toluene (20)	Not dissolved	-	-	-

a) 0.25 mmol *rac*-2-Cl-TA and (–)-ADPE were used for entry 1; 0.5 mmol *rac*-2-Cl-TA and (–)-ADPE were used for entries 2-11.
b) The solvent inclusion was evaluated by TG (entry 1) or ^{1}H NMR analysis (entries 2-10).
c) The yield is based on half the amount of salt considering the amount of solvent included.
d) The ee was determined by HPLC after derivatization to its corresponding methyl ester.
e) Eff. = Yield (%) × ee (%)/10,000.

The crystallization of the diastereomeric salts of *rac*-2-Cl-TA and (–)-ADPE in H$_2$O and 30% EtOH afforded the (*R*)-2-Cl-TA salt with very low resolution efficiencies (entries 1 and 2). In contrast, crystallization in 50% EtOH afforded (*S*)-2-Cl-TA salt accompanied by the incorporation of EtOH with moderate efficiency (entry 3). Similarly, moderate efficiency was observed when MeOH was used as the crystallization solvent, which yielded the (*S*)-2-Cl-TA salt with incorporated solvent. In this case, the enantiopurity increased significantly (entry 4). Crystallization with EtOH produced outstanding results, and afforded the (*S*)-2-Cl-TA salt with

incorporated solvent in high enantiomeric excess as well as overall high efficiency (entry 5). The (*S*)-2-Cl-TA salt was preferentially obtained with good efficiency when *n*-PrOH was employed as the crystallization solvent. The solvent was incorporated in this case also (entry 6). The resolution efficiency obtained from *i*-PrOH was similar to that obtained from *n*-PrOH. However, remarkably, the chirality of 2-Cl-TA in the deposited salt was switched from (*S*) to (*R*), and no solvent was incorporated (entry 7). Similarly, good selectivity for the (*R*)-2-Cl-TA salt was observed when *s*-BuOH was used as the crystallization solvent, but the efficiency value decreased marginally to a moderate value when compared with the case of *i*-PrOH (entry 8). The chirality switching was observed when branched alcohols were employed as solvents for crystallization (on comparing with entries 3, 4, 5 and 6 where linear alcohols have been employed).

Notably, the alcohol solvents were incorporated into the salt crystals when the (*S*)-2-Cl-TA salt was deposited, which implies that solvent incorporation acts as a driving force for chirality switching. THF also afforded the (*R*)-2-Cl-TA salt without being incorporated. However, resolution in THF was less efficient than that in *s*-BuOH (entry 9). Therefore, the (*R*)-2-Cl-TA salt crystals did not contain any incorporated solvent (entries 7, 8, and 9). The solvent 1,4-dioxane did not allow chiral recognition, and the salt did not dissolve when toluene was used as the recrystallization solvent (entries 10 and 11). Notably, linear alcohols such as MeOH, EtOH, and *n*-PrOH yielded the (*S*)-2-Cl-TA salt, whereas branched alcohols such as *i*-PrOH and *s*-BuOH afforded the (*R*)-2-Cl-TA salt, thus switching the chirality. In particular, highly efficient optical resolution was afforded by crystallization in EtOH.

Crystallographic analyses of the diastereomeric salts:

The less-soluble diastereomeric salt, (*S*)-2-Cl-TA · (−)-ADPE, obtained from linear alcohol solutions:

Fig. 3. The (*S*)-2-Cl-TA · (−)-ADPE salt obtained in a 50% EtOH solution, viewed from the *a* axis. The dotted lines indicate hydrogen bonds and the arrows indicate CH/π interactions.

Crystallographic investigations were performed to elucidate the molecular mechanism of chirality switching during the resolution of 2-Cl-TA with (−)-ADPE. Crystals of the diastereomeric salts were prepared from 50% EtOH, MeOH, and *n*-PrOH solutions.

The structure of the needle-like crystal, which was prepared by recrystallization of *rac*-2-Cl-TA · (−)-ADPE in a 50% EtOH solution is shown in Fig. 3. The crystal structure revealed that the solvent was incorporated. The 2-Cl-TA : (−)-ADPE : EtOH ratio was 1 : 1 : 1. The absolute configuration of 2-Cl-TA was inferred to be (*S*), which is consistent with the results

from the resolution (Table 1; entry 3). An array of periodic tubular structures was present along the a axis. The adjacent arrays were organized in an anti-collateral arrangement. A typical columnar hydrogen-bonding network, which was found in other carboxylate salts with enantiopure ADPE[33-37], was constructed with a twofold screw axis (2_1) from (S)-2-Cl-TA and (−)-ADPE. The solvent EtOH molecules were rigidly held in a channel by two hydrogen bonds with the carboxylate oxygen atom of (S)-2-Cl-TA and the hydroxy hydrogen atom of (−)-ADPE, which connected them effectively to the tubular structures. The ammonium hydrogens of (−)-ADPE were linked to the adjacent carboxylate oxygen atoms and the hydroxy oxygen atom of (S)-2-Cl-TA. The solvent incorporation plays a crucial role in the efficient molecular packing of the crystal, and the overall arrangement constitutes a stable non-polar orthorhombic $P2_12_12_1$ crystal, which is attributable to the potent intermolecular interactions. The structure was also reinforced by two CH/π interactions between (S)-2-Cl-TA and (−)-ADPE, which enhanced its stability. The stereoselectivity of (S)-2-Cl-TA was achieved by the fixation of its substituents with intra-array CH/π interactions between the methylene hydrogen atom of (S)-2-Cl-TA and the phenyl group at the 2-position of (−)-ADPE, as well as inter-array CH/π interactions between the para-CH of (S)-2-Cl-TA and the phenyl group substituted at the 1-position of (−)-ADPE [38,39]. From the comparison of XRD patterns, the salt obtained from EtOH solution (Table 1, entry 5) consisted of (S)-2-Cl-TA · (−)-ADPE · EtOH crystal and other crystalline phase, which is probably due to gradual desorption of EtOH from the salt (Fig. 4).
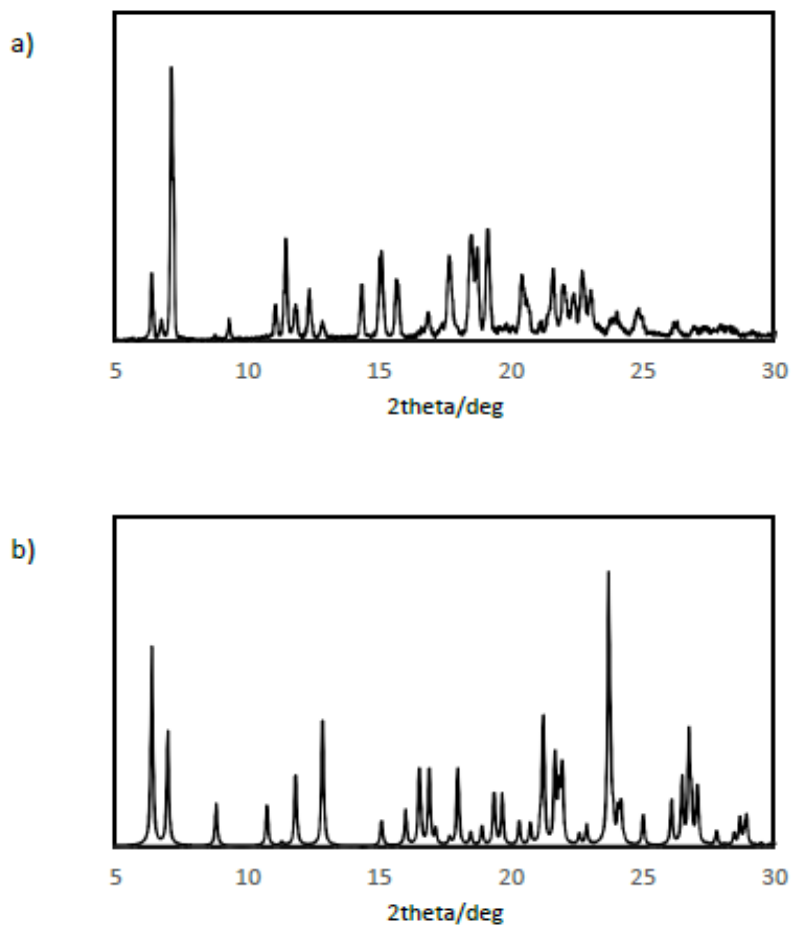
Fig. 4. Powder XRD patterns of a) the salt obtained in EtOH solution (Table 1, entry 5) and

b) (*S*)-2-Cl-TA · (−)-ADPE · EtOH salt simulated from the crystallographic analysis.
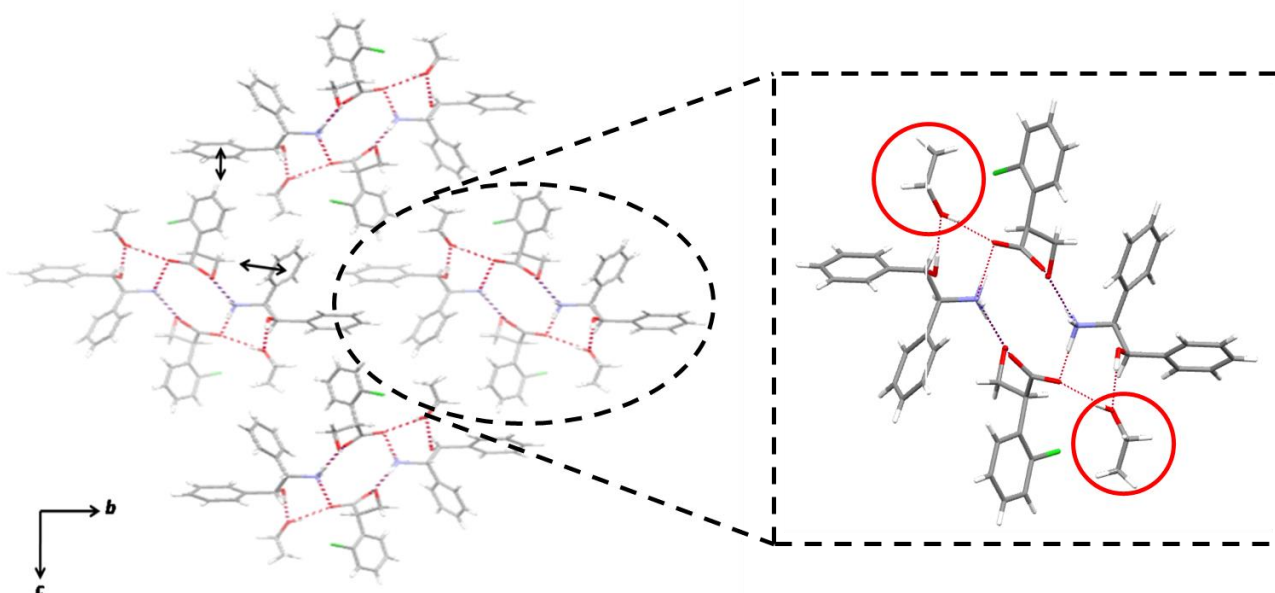
Fig. 5.a. The (*S*)-2-Cl-TA · (−)-ADPE salt obtained in MeOH, viewed from the *a* axis. The

dotted lines indicate hydrogen bonds and the arrows indicate CH/π interactions.
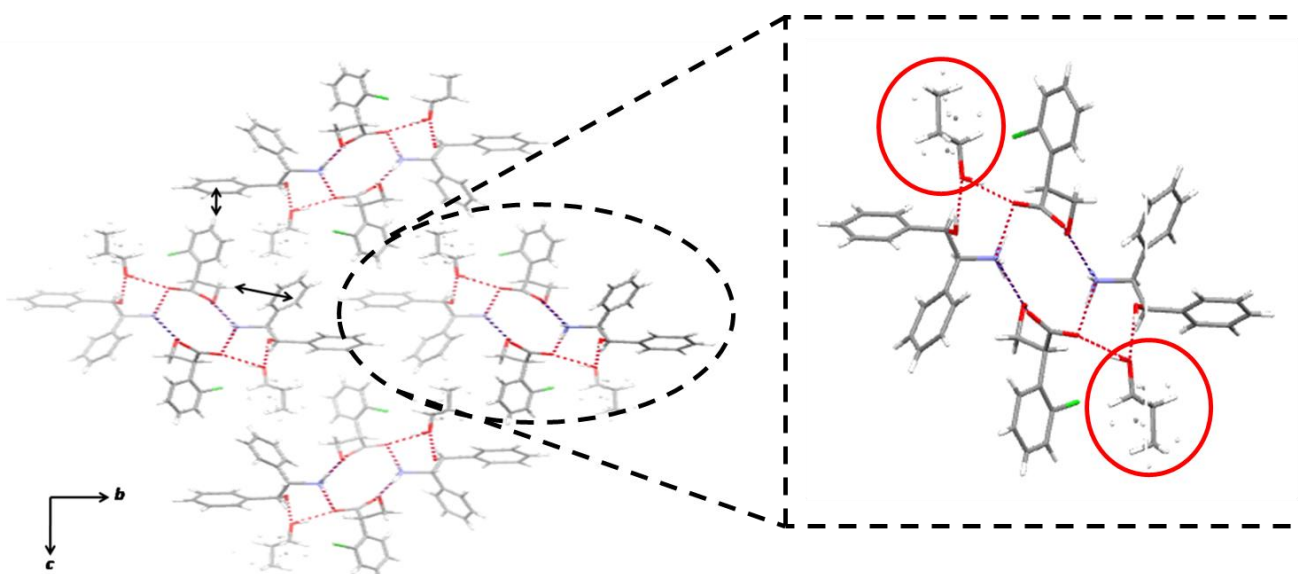
Fig. 5.b. The (*S*)-2-Cl-TA · (−)-ADPE salt obtained in *n*-PrOH, viewed from the *a* axis. The

dotted lines indicate hydrogen bonds and the arrows indicate CH/π interactions.

The structures of the (*S*)-2-Cl-TA · (−)-ADPE diastereomeric salts prepared by recrystallization in MeOH and *n*-PrOH solutions are shown in Fig. 5.a and Fig. 5.b. The linear alcohol solvents were incorporated into both salts, and the structures consisting of arrays of tubular structures were found to be analogous to those of (*S*)-2-Cl-TA · (−)-ADPE · EtOH.

In addition, in the 2-Cl-TA · (−)-ADPE · *n*-PrOH crystals, the *n*-PrOH alkyl chain resembles a disordered structure compared to that of 2-Cl-TA · (−)-ADPE · MeOH and 2-Cl-TA · (−)-ADPE · EtOH crystals. While the two CH/π interactions in the 2-Cl-TA · (−)-ADPE · MeOH crystal were strong, similar to those in the 2-Cl-TA · (−)-ADPE · EtOH crystal, longer CH/π-plane distances showed that they were considerably weaker in the 2-Cl-TA · (−)-ADPE · *n*-PrOH crystal (Table 2). This explains why the stability of the 2-Cl-TA · (−)-ADPE · *n*-PrOH crystal is lower than that of the 2-Cl-TA · (−)-ADPE · MeOH and 2-Cl-TA · (−)-ADPE · EtOH crystals. The 2-Cl-TA · (−)-ADPE · MeOH and 2-Cl-TA · (−)-ADPE · *n*-PrOH crystals exhibited low crystal density (2-Cl-TA · (−)-ADPE · MeOH crystal density = 1.286 g/cm^3; 2-Cl-TA · (−)-ADPE · *n*-PrOH crystal density = 1.296 g/cm^3) compared to the 2-Cl-TA · (−)-ADPE · EtOH crystals, which demonstrated strikingly higher crystal density (1.319 g/cm^3), contributing to a high efficiency result during the resolution (Table 1; entry 5).

Table 2. Summary of the CH/π interactions observed in 2-Cl-TA · (−)-ADPE · MeOH, 2-Cl-TA · (−)-ADPE · EtOH, and 2-Cl-TA · (−)-ADPE · n-PrOH crystals.

Crystal	Type of CH/π interaction	CH----π Plane distance (Å)	C----π Plane distance (Å)
2-Cl-TA · (−)-ADPE · MeOH	Inter CH/π	2.69	3.61
	Intra CH/π	2.84	3.74
2-Cl-TA · (−)-ADPE · EtOH	Inter CH/π	2.75	3.64
	Intra CH/π	2.89	3.76
2-Cl-TA · (−)-ADPE · n-PrOH	Inter CH/π	3.17	4.08
	Intra CH/π	2.96	3.83

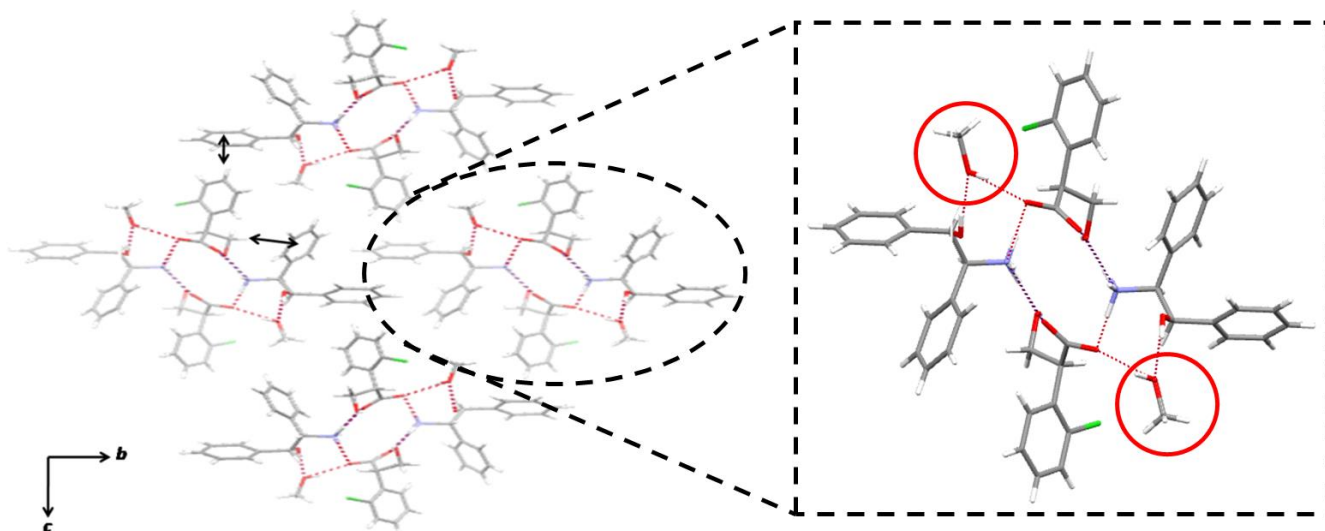**The more-soluble diastereomeric salt, (*R*)-2-Cl-TA · (−)-ADPE, obtained in MeOH:**
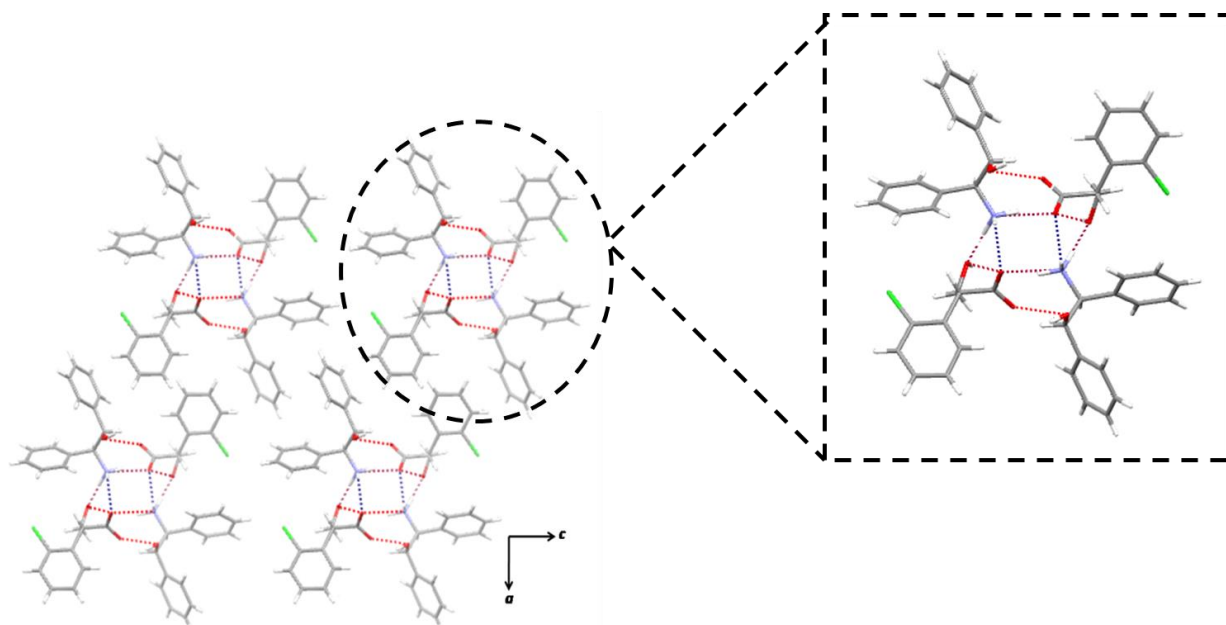
Fig. 6. The (*R*)-2-Cl-TA · (−)-ADPE salt obtained in MeOH, viewed from the *b* axis. The dotted lines indicate hydrogen bonds.

The (*R*)-2-Cl-TA · (−)-ADPE crystal obtained in MeOH was investigated to understand the structure of the more-soluble salt crystallized in MeOH. The structure of the obtained crystals is shown in Fig. 6. They were prepared by recrystallization of *rac*-2-Cl-TA · (−)-ADPE in MeOH. In contrast to the (*S*)-2-Cl-TA · (−)-ADPE crystal structures obtained in MeOH, EtOH, and *n*-PrOH, no solvent incorporation was observed. The ratio of 2-Cl-TA : (−)-ADPE was found to be 1 : 1, and the crystal structure of this salt featured columnar hydrogen-bonding networks. An assembly of the tubular structures was observed. The adjacent structures were positioned parallel to each other. The two carboxylate oxygen atoms of 2-Cl-TA were connected to the hydrogen atoms of the hydroxy group and two ammonium groups of (−)-ADPE via hydrogen bonds. The remaining hydrogen of the ammonium group of (−)-ADPE was

linked to the oxygen of the hydroxy group of another 2-Cl-TA molecule. The entire array is interconnected, forming a tubular structure *via* intermolecular hydrogen bonding. Unlike in the crystal structures of (*S*)-2-Cl-TA · (−)-ADPE · linear alcohol, the π-plane of (−)-ADPE is not perpendicular to the −CH of 2-Cl-TA, and hence no CH/π interactions were present in the crystal to reinforce the structure. The space group of this crystal was determined to be $P2_1$, which is different from the space group observed for the (*S*)-salt crystals obtained in MeOH, EtOH, and *n*-PrOH solutions. The obtained (*R*)-2-Cl-TA · (−)-ADPE crystal structure was deduced to be less stable than the (*S*)-2-Cl-TA · (−)-ADPE · linear alcohol crystal structures, because the lack of solvent incorporation resulted in fewer hydrogen bonds and efficient molecular packing did not occur. The powder XRD pattern of the salt obtained from *i*-PrOH solution during resolution (Table 1, entry 7) was almost consistent with that simulated for the (*R*)-2-Cl-TA · (−)-ADPE salt crystal (Fig. 7).
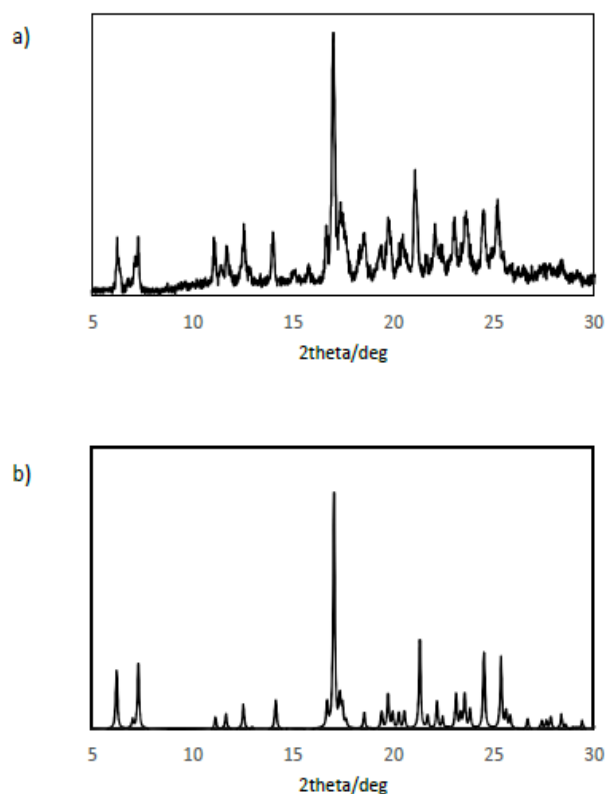
Fig. 7. Powder XRD patterns of a) the salt obtained in *i*-PrOH solution (Table 1, entry7) and b) (*R*)-2-Cl-TA · (−)-ADPE salt simulated from the crystallographic analysis.

The chirality switching mechanism has been elucidated on the basis of the crystal structures of the diastereomeric salts. The solvent was incorporated into the structures of the (*S*)-salt, whereas the (*R*)-salt did not incorporate any solvent. Solvent incorporation in the (*S*)-salt significantly increased its stability compared to that of the (*R*)-salt, leading to chirality switching. In particular, linear alcohols such as MeOH, EtOH, and *n*-PrOH could pack into the narrow channel of the (*S*)-salt crystal, contributing to higher stability by dynamic hydrogen bonding interactions that switch the chirality of 2-Cl-TA. Branched alcohols such as *i*-PrOH and *s*-BuOH could not fill the channel, possibly due to their bulky groups, and thus, afforded the

40

(R)-salt. Considering the above optical resolution results and crystallographic analysis, the order of stability of the diastereomeric 2-Cl-TA salts can be expressed qualitatively as follows:

(S)-2-Cl-TA · (–)-ADPE · linear alcohol > (R)-2-Cl-TA · (–)-ADPE > (S)-2-Cl-TA · (–)-ADPE.
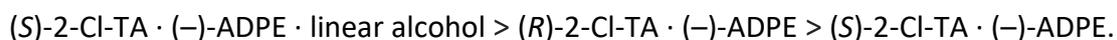
These results contrast interestingly with our previous resolution results for TA. In the case of TA, both the linear and branched alcohols (EtOH and *i*-PrOH solutions) filled the channel of the salt crystal, affording the solvent incorporated (S)-TA salt. But the presence of a bulky chlorine substituent in 2-Cl-TA narrowed the channel gap of the salt meaning it could only be filled with linear alcohols. Therefore, only linear alcohols yielded a solvent incorporated (S)-2-Cl-TA salt and the branched alcohols could not afford the (S)-2-Cl-TA salt.

Optical resolution of *rac*-3-Cl-TA and *rac*-4-Cl-TA with (1*R*,2*S*)-(–)-ADPE:

The effects of the solvents employed for recrystallization during the optical resolution of *rac*-3-Cl-TA and *rac*-4-Cl-TA with (–)-ADPE were investigated. The experimental procedure was the same as that for 2-Cl-TA (Tables 3 and 4).

Table 3: Optical resolution of *rac*-3-Cl-TA with (–)-ADPE[a]

Entry	Recrystallization solvent (mL)	Ratio of the salt to solvent included [b]	Yield % [c]	Ee % [d]	Eff. [e]
1	H$_2$O (5.5)	Not included	94.4	7 (R)	0.07
2	EtOH (5)	Not included	98.5	*rac.*	0
3	*i*-PrOH(2.5)	Not included	89.7	*rac.*	0
4	1,4-dioxane (2.5)	Not included	43.7	5 (R)	0.02

a) 0.5 mmol *rac*-3-Cl-TA and (–)-ADPE were used for entry 2; 0.25 mmol *rac*-3-Cl-TA and (–)-ADPE were used for entries 1, 3 and 4.
b) The solvent inclusion was evaluated by TG (entry 1) or ^{1}H NMR analysis (entries 2-4).
c) The yield is based on half the amount of salt.
d) The ee was determined by HPLC after derivatization to its corresponding methyl ester.
e) Eff. = Yield (%) × ee (%)/10,000.

Crystallization of the diastereomeric salts of *rac*-3-Cl-TA and (–)-ADPE in H_2O resulted

in (*R*)-3-Cl-TA salt with very low-resolution efficiency (entry 1). The resolutions indicated that

EtOH and *i*-PrOH (entries 2 and 3) produced almost racemic mixtures, while 1,4-dioxane

afforded the (*R*)-3-Cl-TA salt with very low efficiency (entry 4). There was no solvent

incorporated into any of these salts (entries 2-4).

Table 4: Optical resolution of racemic *rac*-4-Cl-TA with (–)-ADPE[a]

Entry	Recrystallization solvent (mL)	Ratio of the salt to solvent included [b]	Yield % [c]	Ee % [d]	Eff. [e]
1	H_2O (9)	1:2	87.9	20 (*S*)	0.18
2	MeOH (3.5)	Not included	67.8	*rac.*	0
3	EtOH (18)	Not included	42.3	*rac.*	0
4	*i*-PrOH (14)	Not included	98.0	*rac.*	0
5	THF (20)	Not included	86.5	*rac.*	0
6	1,4-dioxane (17)	Not included	95.2	*rac.*	0
7	Toluene (37.5)	Not dissolved	-	-	-
8	$CHCl_3$(36)	Not dissolved	-	-	-

a) 0.25 mmol *rac*-4-Cl-TA and (–)-ADPE were used for entry 1; 0.5 mmol *rac*-4-Cl-TA and (–)-ADPE were used for entries 2-8.
b) The solvent inclusion was evaluated by TG (entry 1) or ^1H NMR analysis (entries 2-6).
c) The yield is based on half the amount of salt considering the amount of solvent included.
d) The ee was determined by HPLC after derivatization to its corresponding methyl ester.
e) Eff. = Yield (%) × ee (%)/10,000.

The crystallization of the diastereomeric salts of *rac*-4-Cl-TA and (–)-ADPE from H_2O

afforded (*S*)-4-Cl-TA salt accompanied by the incorporation of H_2O with moderate efficiency

(entry 1). Almost racemic mixtures were obtained when resolution was attempted in some

solvents (entries 2–6). However, the salt was not soluble in toluene and $CHCl_3$ (entries 7 and

8). Therefore, chirality switching could not be achieved in the case of 3-Cl-TA and 4-Cl-TA.

Crystallographic analysis of the diastereomeric salt, *rac*-4-Cl-TA · (–)-ADPE, and the influence of the position of the chlorine substituent on solvent-induced chirality switching:
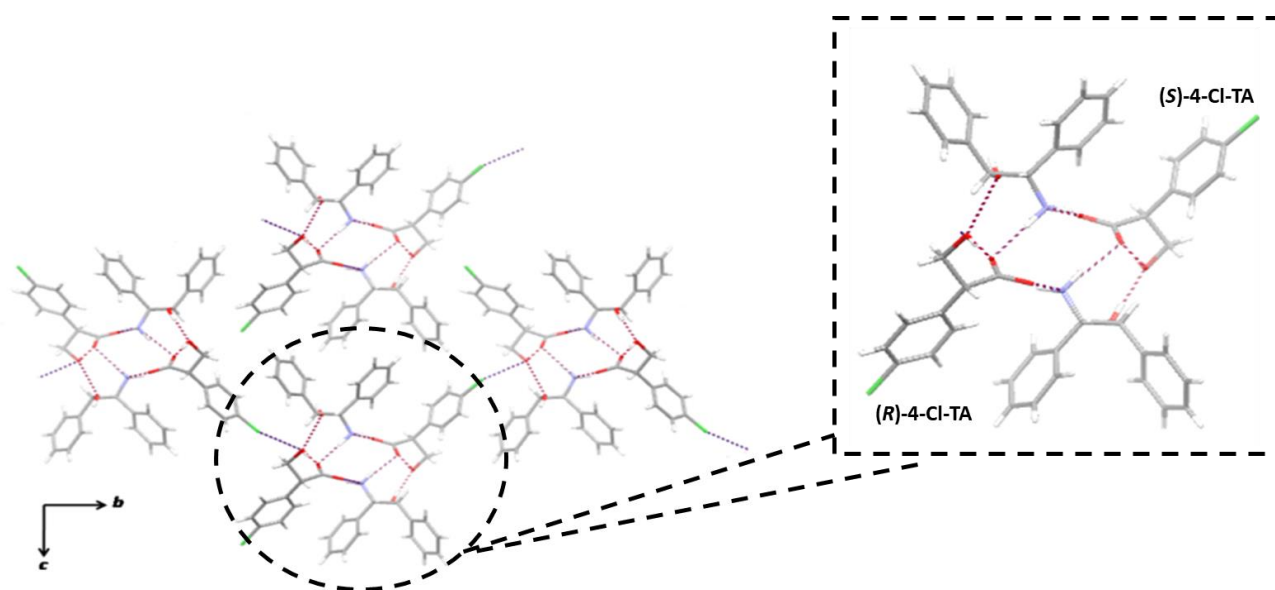
Fig. 8. The *rac*-4-Cl-TA · (–)-ADPE salt obtained in *i*-PrOH solution, viewed from the *a* axis. The dotted lines indicate hydrogen bonds.

The structure of the crystal prepared from *rac*-4-Cl-TA · (–)-ADPE in *i*-PrOH is shown in Fig. 8. The crystal structure revealed no solvent incorporation. Both enantiomers, (*S*)-4-Cl-TA and (*R*)-4-Cl-TA, were present in a ratio of 1 : 1. Therefore, the enantiopurity of 4-Cl-TA was confirmed to be racemic, which is consistent with the resolution results (Table 4, entry 4). The ratio of *rac*-4-Cl-TA : (–)-ADPE was found to be 1 : 1. An array of periodic tubular structures, similar to that found in the 2-Cl-TA salts, was present. The carboxylate oxygens of 4-Cl-TA form hydrogen bonds with the adjacent ammonium hydrogens of (–)-ADPE. The hydroxy hydrogen of (–)-ADPE is also linked with the neighboring oxygen atom of the hydroxy group of 4-Cl-TA. The overall arrangement constitutes a monoclinic $P2_1$ crystal system. No CH/π interactions reinforced the crystal structure. Furthermore, inter-array hydrogen bonding is observed between the chlorine atom in the *para* position of the (*S*)-4-Cl-TA molecule and the

hydroxy hydrogen of the (*R*)-4-Cl-TA molecule. From Table 4, entry 1, H_2O afforded the (*S*)-salt. So probably, the (*S*)-4-Cl-TA · (−)-ADPE crystal obtained from H_2O would be different from this crystal.

The tubular structure consists of a channel space that facilitated the entry of solvent molecules which reinforced the supramolecular structure of the salt thereby contributing to chirality switching in 2-Cl-TA. Furthermore, the position of the chlorine substituent plays an important role in chirality switching. It is likely that when the chlorine substituent is in the *ortho* position, it is directed toward the tubular structure, which favors molecular packing, resulting in efficient chirality switching in 2-Cl-TA. However, when the chlorine substituent is in the *meta* and *para* positions, it is directed outside the tubular structure, which disrupts the packing, thus hindering the chirality switching effect in 3-Cl-TA and 4-Cl-TA. In addition, the chlorine substituent at the *meta* and *para* positions probably contributed to the formation of Cl----H-O hydrogen bonds. This would have limited the space of the channel in the crystal, thus blocking the entry of solvent molecules, which inhibited the solvent-induced chirality switching effect in 3-Cl-TA and 4-Cl-TA.

2.3 Conclusion:

Solvent-induced chirality switching, in the optical resolution of chlorine-substituted TAs with (–)-ADPE has been demonstrated. In the case of 2-Cl-TA, resolution in branched alcohols such as *i*-PrOH and *s*-BuOH afforded (*R*)-2-Cl-TA · (–)-ADPE as a less-soluble diastereomeric salt, whereas the (*S*)-2-Cl-TA · (–)-ADPE salt was obtained in linear alcohols such as MeOH, EtOH, and *n*-PrOH. The stereoselectivity could be switched by employing different types of solvents. The crystal structures of both the diastereomeric salts were revealed, and the incorporation of solvent into the (*S*)-2-Cl-TA salt contributed to its stability. Solvent-induced chirality switching could not be achieved with 3-Cl-TA and 4-Cl-TA. The structural effect associated with changing the position of the chlorine substituent from the *ortho* to the *meta* or *para* position on solvent-induced chirality switching is also discussed. This study provides an unsophisticated technique for accessing both enantiomers without changing the resolving agent.

2.4 Experimental section:
2.4.1 General methods:

All the reagents and solvents were purchased and used as received. All ^{1}H NMR and ^{13}C NMR spectra were recorded on Bruker AVANCE 300, 400 or 500 MHz spectrometer. IR spectra were measured on a JASCO FT/IR-4600 spectrometer. Melting points were recorded on a MEL-TEMP apparatus and reported uncorrected. The enantiomeric excess values were determined by chiral HPLC analyses (Daicel Chiralcel OD-3 column; Eluent: 10% *i*-PrOH in hexane; Flow rate: 1.0 mL/min or 0.5 mL/min). Mass spectra was analyzed using Bruker Autoflex III mass spectrometer.

2.4.2 Synthesis of chlorine-substituted TAs:

Synthesis of *rac*-2-Cl-TA methyl ester: To a stirred solution of 2-chlorophenylacetic acid methyl ester (3.02 g, 16.4 mmol) in DMSO (33 mL), sodium ethoxide (0.0661 g, 0.971 mmol) and paraformaldehyde (0.530 g, 17.6 mmol) were added at 0 °C and the reaction mixture was stirred at room temperature for 25 h under a N_2 atmosphere. The reaction mixture was then diluted with EtOAc (100 mL), washed with water (3 X 30 mL) and brine (30 mL). The organic phase was dried over anhydrous Na_2SO_4 and evaporated under vacuum. Finally the crude product was purified by silica gel column chromatography (eluent; hexane : ethyl acetate = 10 : 1) and obtained as colorless oil (2.85 g, 13.3 mmol). The yield was calculated to be 81.2%.
^1H NMR (300 MHz, CDCl$_3$): δ (ppm) 7.49-7.35 (m, 1H), 7.30-7.15 (m, 3H), 4.38 (dd, J_1=8.4 Hz, J_2=4.5 Hz, 1H), 4.10 (dd, J_1= 11.4 Hz, J_2= 8.4 Hz, 1H), 3.83 (dd, J_1= 11.4 Hz, J_2= 4.8 Hz, 1H), 3.74 (s, 3H). ^{13}C NMR (125 MHz, CDCl$_3$): δ (ppm) 173.6, 134.2, 133.7, 130.1, 129.5, 129.1, 127.3, 63.4, 52.5, 50.5. IR (neat): ν(cm^{-1}) 3435, 2952, 2885, 1734, 1475, 1436, 1353, 1131, 1041, 754, 693. MALDI-TOF-MS: *m/z* = 237.08 and 239.07 [M+Na]$^+$ (calcd. For $C_{10}H_{11}ClO_3$+Na = 237.03 and 239.03).

Synthesis of *rac*-2-Cl-TA: To a stirred solution of 2-Cl-TA methyl ester (2.85 g, 13.3 mmol) in THF (39.7 mL), lithium hydroxide monohydrate (1.39 g, 33.1 mmol) in water (11.4 mL) was added dropwise at 0 °C. The reaction mixture was stirred at room temperature for 2.5 h. It was acidified with 2N aqueous HCl (pH ~ 3) and extracted with chloroform (30 mL X 3). The combined organic layers were washed with brine (25 mL), dried over anhydrous Na_2SO_4 and evaporated under vacuum. Finally the crude product was recrystallized from toluene and *rac*-2-Cl-TA was obtained as a white solid (2.01 g, 10.0 mmol). The yield was calculated to be

75.4%. Mp. 92-93 °C. ^{1}H NMR (300 MHz, CDCl$_3$/CD$_3$OD): δ (ppm) 7.58-7.09 (m, 4H), 4.37 (dd, J_1= 8.4 Hz, J_2= 4.8 Hz, 1H), 4.06 (dd, J_1= 11.4 Hz, J_2= 8.4 Hz, 1H), 3.82 (dd, J_1= 11.4 Hz, J_2= 4.8 Hz, 1H). ^{13}C NMR (125 MHz, CDCl$_3$/CD$_3$OD): δ (ppm) 175.0, 134.2, 134.0, 129.9, 129.4, 128.9, 127.2, 63.1, 50.3. IR (KBr): ν(cm^{-1}) 3357, 2948, 1706, 1474, 1415, 1251, 1234, 1192, 1129, 1038, 945, 750, 680. MALDI-TOF-MS: *m/z* = 223.11 and 225.11 [M+Na]$^+$ (calcd. For C$_9$H$_9$ClO$_3$+Na = 223.01 and 225.01).

Synthesis of *rac*-3-Cl-TA methyl ester: The same procedure has been followed as in the synthesis of *rac*-2-Cl-TA methyl ester. The starting material employed was 3-chlorophenylacetic acid methyl ester. The product was purified by silica gel column chromatography (eluent; hexane : ethyl acetate = 10 : 1) and obtained as colorless oil. Yield 51.8%. ^{1}H NMR (300 MHz, CDCl$_3$): δ (ppm) 7.34-7.22 (m, 3H), 7.20-7.10 (m, 1H), 4.20-4.02 (m, 1H), 3.89-3.77 (m, 2H), 3.73 (s, 3H). ^{13}C NMR (125 MHz, CDCl$_3$): δ (ppm) 173.0, 137.5, 134.7, 130.1, 128.4, 128.0, 126.4, 64.4, 53.5, 52.4. IR (neat): ν(cm^{-1}) 3436, 2953, 2885, 1736, 1596, 1574, 1477, 1433, 1200, 1169, 1083, 1044, 772, 700. MALDI-TOF-MS: *m/z* = 237.14 and 239.14 [M+Na]$^+$ (calcd. For C$_{10}$H$_{11}$ClO$_3$+Na = 237.03 and 239.03).

Synthesis of *rac*-3-Cl-TA: The same procedure has been followed as in the synthesis of *rac*-2-Cl-TA. The product was purified by recrystallization from toluene and obtained as a white solid. Yield 47.0%. Mp. 74-75°C. ^{1}H NMR (300 MHz, CDCl$_3$/CD$_3$OD): δ (ppm) 7.39-7.12 (m, 4H), 4.16-4.00 (m, 1H), 3.89-3.74 (m, 2H).^{13}C NMR (125 MHz, CDCl$_3$/CD$_3$OD): δ (ppm) 174.8, 138.3,134.7, 130.2, 128.6, 128.0, 126.8, 64.2, 53.9. IR (KBr): ν(cm^{-1}) 3375, 2954, 1693, 1572, 1434, 1327, 1246, 1183, 1065, 1042, 951, 768, 696. MALDI-TOF-MS: *m/z* =223.10 and 225.10 [M+Na]$^+$ (calcd. For C$_9$H$_9$ClO$_3$+Na = 223.01 and 225.01).

Synthesis of *rac*-4-Cl-TA methyl ester: The same procedure has been followed as in the synthesis of *rac*-2-Cl-TA methyl ester. The starting material employed was 4-chlorophenylacetic acid methyl ester. The product was purified by silica gel column chromatography (eluent; hexane : ethyl acetate = 10 : 1) and obtained as colorless oil. Yield 66.9%. ^{1}H NMR (300 MHz, CDCl$_3$): δ (ppm) 7.39-7.16 (m, 4H), 4.18-4.02 (m, 1H), 3.89-3.77 (m, 2H), 3.71 (s, 3H). ^{13}C NMR (125 MHz, CDCl$_3$): δ (ppm) 173.4, 134.2, 133.9, 129.7, 129.2, 64.5, 53.3, 52.5. IR (neat): ν(cm^{-1}) 3436, 2952, 2884, 1735, 1493, 1437, 1349, 1254, 1200, 1169, 1092, 1043, 1015, 827, 764, 717, 526, 456. MALDI-TOF-MS: *m/z* = 237.15 and 239.17 [M+Na]$^+$ (calcd. For C$_{10}$H$_{11}$ClO$_3$+Na = 237.03 and 239.03).

Synthesis of *rac*-4-Cl-TA: The same procedure has been followed as in the synthesis of *rac*-2-Cl-TA. The product was purified by recrystallization from H$_2$O and obtained as white solid. Yield 79.1%. Mp. 142-143 °C. ^{1}H NMR (300 MHz, CDCl$_3$/CD$_3$OD): δ (ppm) 7.45-7.19 (m, 4H), 4.07 (dd, J_1 = 12.3 Hz, J_2 = 10.2 Hz, 1H), 3.90-3.68 (m, 2H). ^{13}C NMR (125 MHz, CDCl$_3$/CD$_3$OD): δ (ppm) 175.2, 134.9, 133.8, 129.9, 129.1, 64.4, 53.6. IR (KBr): ν(cm^{-1}) 3206, 2945, 1694, 1494, 1410, 1296, 1283, 1244, 1221, 1093, 1041, 1009, 849, 819, 757, 715, 667, 513, 463. MALDI-TOF-MS: *m/z* = 223.08 and 225.08 [M+Na]$^+$ (calcd. For C$_9$H$_9$ClO$_3$+Na = 223.01 and 225.01).

2.4.3 Optical resolution of chlorine-substituted TAs with (1*R*,2*S*)-(–)-ADPE:

The resolution experiment in the case of 2-Cl-TA was carried out as follows: Equimolar amounts of *rac*-2-Cl-TA and (–)-ADPE were dissolved in methanol followed by evaporation under vacuum. After concentration, the resulting white solid was recrystallized from a

suitable solvent. The obtained crystals were filtered; dried overnight and characterized by TG or ^{1}H NMR analysis. The apparent yield was calculated based on half the amount of salt considering the solvent included. A small portion of the salt was decomposed by the addition of 1N aqueous HCl solution and extracted with diethyl ether. The organic phase was collected and washed with water. Further it was dried over anhydrous Na_2SO_4 and concentrated to obtain 2-Cl-TA. After derivatizing the 2-Cl-TA to its corresponding methyl ester by employing TMSCHN$_2$, chiral HPLC analysis was performed (Daicel Chiralcel OD-3, eluent: 10% *i*-PrOH in hexane, flow rate: 1.0 mL/min). 2-Cl-TA methyl ester: $t_r(R)$ = 7.9 min, $t_r(S)$ = 9.1 min. As typical examples, for entry 5 in Table 1, *rac*-2-Cl-TA (0.101 g) and (−)-ADPE (0.108 g) were used and the salt was recrystallized from EtOH (7 mL) to give the salt (0.0879 g) as needle-like crystals. $[\alpha]^{20}_{589}$ = −84.4° (c 0.505, MeOH); for entry 7, *rac*-2-Cl-TA (0.100 g) and (−)-ADPE (0.108 g) were used and the salt was recrystallized from *i*-PrOH (3.5 mL) to give the salt (0.0745 g) as a white solid. $[\alpha]^{20}_{589}$ = −66.7° (c 0.390, MeOH). The same procedure has been followed for the optical resolution of *rac*-3-Cl-TA and *rac*-4-Cl-TA. 3-Cl-TA methyl ester: $t_r(R)$ = 7.6 min, $t_r(S)$ = 8.8 min. 4-Cl-TA methyl ester: $t_r(R)$ = 8.0 min, $t_r(S)$ = 8.7 min.

2.4.4 Single crystal X-ray analyses of the diastereomeric salt crystals:

Single crystals suitable for X-ray diffraction analysis were prepared by slow evaporation of the saturated solutions of racemic diastereomeric salts, except in the case of (*S*)-2-Cl-TA · (—)-ADPE · *n*-PrOH where partially resolved (*S*)-2-Cl-TA · (—)-ADPE salt was employed. X-ray crystallographic data were collected on a Bruker Smart APEX II diffractometer with graphite monochromated Mo-Kα radiation. The structures were solved by a direct method using SIR 2014 and refined by SHELXL-2018 program.[40] Crystal data for (*S*)-2-Cl-TA · (—)-ADPE · EtOH: $C_{25}H_{30}ClNO_5$, M = 459.95, orthorhombic, *a* = 5.653(2), *b* =

16.361(6), c = 25.036(10) Å, V = 2315.6(15) Å^3, T = 150 K, space group $P2_12_12_1$, Z = 4, 13752

reflections measured, 5338 independent reflections (R_{int} = 0.0869), The final R_1 was 0.0633 (I

> 2σ(I)) and wR(F$_2$) was 0.1387 (I > 2σ(I)), CCDC: 2113378. Crystal data for (*S*)-2-Cl-TA · (—)-

ADPE · MeOH: C$_{24}$H$_{28}$ClNO$_5$, M = 445.92, orthorhombic, a = 5.6306(8), b = 16.341(2), c =

25.037(4) Å, V = 2303.7(6) Å^3, T = 150 K, space group $P2_12_12_1$, Z = 4, 13596 reflections

measured, 5283 independent reflections (R_{int} = 0.1926), The final R_1 was 0.0600 (I > 2σ(I)) and

wR(F$_2$) was 0.1391 (I > 2σ(I)), CCDC: 2113379. Crystal data for (*S*)-2-Cl-TA · (—)-ADPE · *n*-PrOH:

C$_{26}$H$_{32}$ClNO$_5$, M = 473.97, orthorhombic, a = 5.6922(13), b = 16.573(4), c = 25.742(6) Å, V =

2428.4(10) Å^3, T = 150 K, space group $P2_12_12_1$, Z = 4, 14387 reflections measured, 5611

independent reflections (R_{int} = 0.2159), The final R_1 was 0.0729 (I > 2σ(I)) and wR(F$_2$) was

0.1535 (I > 2σ(I)), CCDC: 2113380. Crystal data for (*R*)-2-Cl-TA · (—)-ADPE: C$_{23}$H$_{24}$ClNO$_4$, M =

413.88, monoclinic, a = 13.589(3), b = 5.5760(11), c = 15.320(3) Å, β = 113.456(3)°, V =

1064.9(4) Å^3, T = 150 K, space group $P2_1$, Z = 2, 6297 reflections measured, 4299 independent

reflections (R_{int} = 0.1331), The final R_1 was 0.0987 (I > 2σ(I)) and wR(F$_2$) was 0.2416 (I > 2σ(I)),

CCDC: 2113381. Crystal data for *rac*-4-Cl-TA · (—)-ADPE: C$_{23}$H$_{24}$ClNO$_4$, M = 413.88, monoclinic,

a = 5.4164(13), b = 25.111(6), c = 14.782(3) Å, β = 94.035(3)°, V = 2005.5(8) Å^3, T = 150 K, space

group $P2_1$, Z = 4, 11807 reflections measured, 8446 independent reflections (R_{int} = 0.1624),

The final R_1 was 0.0688 (I > 2σ(I)) and wR(F$_2$) was 0.1636 (I > 2σ(I)), CCDC: 2113382.

2.5 References:

1. Jacques, J.; Collet, A.; Wilen, S. H. *Enantiomers, Racemates, and Resolutions*; Wiley & Sons: New York, NY, 1981.

2. Kozma, D. *Optical Resolutions via Diastereomeric Salt Formation*; CRC: London, 2002.

3. Faigl, F.; Fogassy, E.; Nógrádi, M.; Pálovics, E.; Schindler, J. *Tetrahedron: Asymmetry* **2008**, *19*, 519-536.

4. Siedlecka, R. *Tetrahedron* **2013**, *69*, 6331-6363.

5. Karamertzanis, P. G.; Anandamanoharan, P. R.; Fernandes, P.; Cains, P. W.; Vickers, M.; Tocher, D. A.; Florence, A. J.; Price, S. L. *J. Phys. Chem. B* **2007**, *111*, 5326-5336.

6. Bereczki, L.; Bombicz, P.; Balint, J.; Egri, G.; Schindler, J.; Pokol, G.; Fogassy, E.; Marthi, K. *Chirality* **2009**, *21*, 331-338.

7. Palovics, E.; Schindler, J.; Faigl, F.; Fogassy, E. *Tetrahedron: Asymmetry* **2010**, *21*, 2429-2434.

8. He, Q.; Rohani, S.; Zhu, J.; Gomaa, H. *Chirality* **2012**, *24*, 119-128.

9. Wang, P.; Zhang, E.; Niu, J.; Ren, Q.; Zhao, P.; Liu, H. *Tetrahedron: Asymmetry* **2012**, *23*, 1046-1051.

10. Kodama, K.; Hayashi, N.; Yoshida, Y.; Hirose, T. *Tetrahedron* **2016**, *72*, 1387–1394.

11. Sakai, K.; Sakurai, R.; Hirayama, N. *Top. Curr. Chem.* **2007**, *269*, 199–231.

12. Taniguchi, K.; Aruga, M.; Yasutake, M.; Hirose, T. *Org. Biomol. Chem.* **2008**, *6*, 458–463.

13. Sakurai, R.; Sakai, K.; Kodama, K.; Yamaura, M. *Tetrahedron: Asymmetry* **2012**, *23*, 221–224.

14. Schmitt, M.; Schollmeyer, D.; Waldvogel, S. R. *Eur. J. Org. Chem.* **2014**, 1007–1012.

15. Caldwell, HC.; Finkelstein, JA.; Arbazov, D.; Pelikan, C.; Groves, WG. *J. Med. Chem.* **1969**, *12*, 477–480.

16. Dei, S.; Bartolini, A.; Bellucci, C.; Ghelardini, C.; Gualtieri, F.; Manetti, D.; Romanelli, M. N.; Scapecchi, S.; Teodori, E. *Eur. J. Med. Chem.* **1997**, *32*, 595-605.

17. Leete, E.; Kowanko, N.; Newmark, A. R. *J. Am. Chem. Soc.* **1975**, *97*, 6826-6830.

18. Leete, E. *J. Am. Chem. Soc.* **1984**, *106*, 7271-7272.

19. Gualtieri, F.; Conti, G.; Dei, S.; Giovannoni, M. P.; Nannucci, F.; Romanelli, M. N.; Scapecchi, S.; Teodori, E.; Fanfani, L.; Ghelardini, C.; Giotti, A.; Bartolini, A. *J. Med. Chem.* **1994**, *37*, 1704-1711.

20. O'Hagan, D.; Robins, R. *Chem. Soc. Rev.* **1998**, *27*, 207-212.

21. Atuu, M. R.; Mahmood, S. J.; Laib, F.; Hossain, M. M. *Tetrahedron: Asymmetry* **2004**, *15*, 3091-3101.

22. Klomp, D.; Peters, J. A.; Hanefeld, U. *Tetrahedron: Asymmetry* **2005**, *16*, 3892-3896.

23. Atuu, M. R.; Hossain, M. M. *Tetrahedron Lett.* **2007**, *48*, 3875-3878.

24. Wang, P.; Tsai, S. *J. Mol. Catal. B: Enzym.* **2009**, *57*, 158-163.

25. McKenzie, A.; Wood, J. K. *J. Chem. Soc.* **1919**, *115*, 828-840.

26. King, H.; Palmer, A. D. *J. Chem. Soc.* **1922**, *121*, 2577-2586.

27. Fodor, G.; Rakoczi, J.; Csepreghy, G. Y. *Acta Chim. Hung.* **1961**, *28*, 409-411.

28. King, H. *J. Chem. Soc.* **1919**, *115*, 476-508.

29. Kodama, K.; Kurozumi, N.; Shitara, H.; Hirose, T. *Tetrahedron* **2014**, *70*, 7923–7928.

30. Kodama, K.; Shitara, H.; Hirose, T. *Cryst. Growth Des.* **2014**, *14*, 3549–3556.

31. Shitara, H.; Shintani, T.; Kodama, K.; Hirose, T. *J. Org. Chem.* **2013**, *78*, 9309–9316.

32. Kodama, K.; Kawasaki, K.; Yi, M.; Tsukamoto, K.; Shitara, H.; Hirose, T. *Cryst. Growth Des.* **2019**, *19*, 7153–7159.

33. Kinbara, K.; Kobayashi, Y.; Saigo, K. *J. Chem. Soc., Perkin Trans. 2* **1998**, 1767-1775.

34. Kodama, K.; Kobayashi, Y.; Saigo, K. *Chem.—Eur. J.* **2007**, *13*, 2144-2152.

35. Kodama, K.; Kobayashi, Y.; Saigo, K. *Cryst. Growth Des.* **2007**, *7*, 935-939.

36. Kobayashi, Y.; Soetrisno; Kodama, K.; Saigo, K. *Tetrahedron: Asymmetry* **2008**, *19*, 295-301.

37. Shiota, N.; Kinuta, T.; Sato, T.; Tajima, N.; Kuroda, R.; Matsubara, Y.; Imai, Y. *Cryst. Growth Des.* **2010**, *10*, 1341-1345.

38. Suezawa, H.; Ishihara, S.; Umezawa, Y.; Tsuboyama, S.; Nishio, M. *Eur. J. Org. Chem.* **2004**, *2004*, 4816−4822.

39. Yoji, U.; Sei, T.; Kazumasa, H.; Jun, U.; Motohiro, N. *Bull. Chem. Soc. Jpn.* **1998**, *71*, 1207−1213.

40. Sheldrick, G. M. *Acta Cryst.* **2015**, *C71*, 3-8.

CHAPTER 3

**Enantioseparation of 3-Hydroxy-5-phenylpentanoic acid
via Diastereomeric Salt Formation**

3.1 Introduction:

Optically pure hydroxycarboxylic acids are important compounds that can be widely employed as chiral precursors because their functional groups can be easily modified. Among the hydroxycarboxylic acids, enantiopure 3-hydroxycarboxylic acids have received considerable attention as they have been proven to be valuable synthons and can be used as starting materials in the synthesis of antibiotics, beta-amino acids, vitamins, flavors, and pheromones.[1-4] They are also vital subunits[5] of polyketide natural products, such as amphotericin B,[6] tylosin,[7] and rosaramicin.[8] Moreover, several optically pure 3-hydroxycarboxylic acids exhibit critical biological activities, such as antimicrobial and antiviral potential. For example, (R)-3-hydroxy-5-phenylpentanoic acid can effectively attack *Listeria monocytogenes*, a species of pathogenic bacteria that causes listeriosis.[9,10]

Basic resolving agents, such as cinchonidine[11-13] and ADPE,[14-16] have been used to resolve racemic hydroxycarboxylic acids. Previously, we reported the optical resolution of 3-hydroxypropionic acids (3-hydroxy-2-phenylpropionic acid, 3-hydroxy-2-(chlorophenyl)propionic acids, and 3-hydroxy-3-phenylpropionic acid) with (−)-ADPE. Crystallographic investigation revealed that hydrogen bonding and CH/π interactions play a crucial role in chiral recognition by reinforcing the supramolecular structure of the salt.[17-19] To expand the substrate scope to other 3-hydroxycarboxylic acids with a more flexible substituent at the stereogenic center, we investigated the enantioseparation of racemic 3-hydroxy-4-phenylbutanoic acid (*rac*-**1**), and 3-hydroxy-4-(4-chlorophenyl)butanoic acid (*rac*-**2**) with ADPE and cinchonidine *via* diastereomeric salt formation. The above mentioned target compounds, *rac*-**1** and *rac*-**2** were resolved successfully and efficiently by ADPE and cinchonidine. We also investigated the enantioseparation of racemic 3-hydroxy-5-

phenylpentanoic acid (*rac*-**3**) with (−)-ADPE. Although *rac*-**3** was resolved by (−)-ADPE, the maximum resolution efficiency was not high (32 %).

Therefore, in order to improve the resolution efficiency of *rac*-**3**, we investigated the enantioseparation of *rac*-**3** with cinchonidine via diastereomeric salt formation in this study. The reason for selecting cinchonidine as the resolving agent for *rac*-**3** is that, cinchonidine gave efficient results during the resolution of other 3-hydroxycarboxylic acids, *rac*-**1** and *rac*-**2**. Moreover, cinchonidine, being an inexpensive resolving agent, is rigid and bulky and has resolved flexible β-chiral 3-hydroxycarboxylic acids. Herein, we demonstrate the efficient optical resolution of *rac*-**3**, and the chiral recognition was elucidated by analyzing the crystal structures of diastereomeric salt.
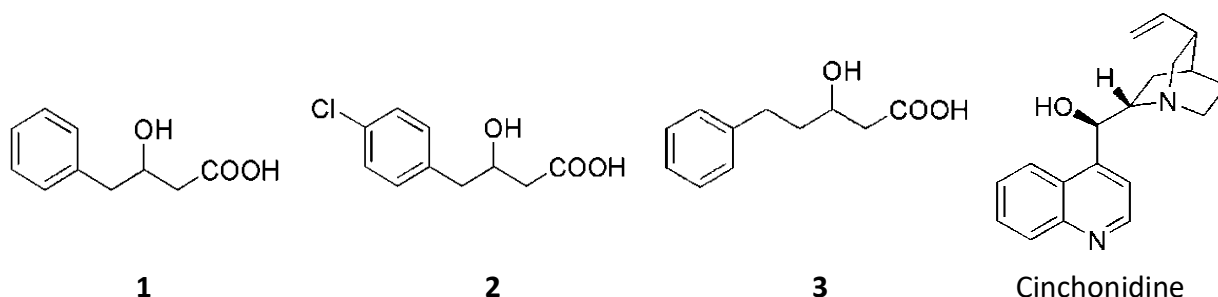
Fig. 1. Chemical structures of racemic 3-hydroxycarboxylic acids and cinchonidine.

3.2 Results and Discussion:

Synthesis of racemic 3-hydroxy-5-phenylpentanoic acid (*rac*-3) using Reformatsky

reaction:

Racemic 3-hydroxy-5-phenylpentanoic acid (*rac*-**3**) has been synthesized using Reformatsky reaction (Scheme. 1) and utilized for the optical resolution experiments. The detailed experimental procedure for the synthesis of *rac*-**3** has been mentioned in the experimental section.
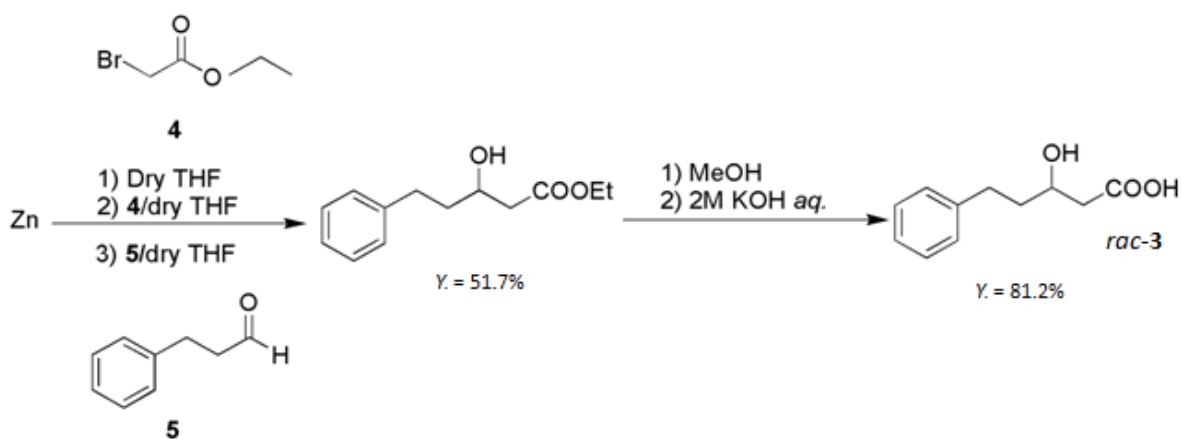
Scheme. 1. Synthesis of racemic 3-hydroxy-5-phenylpentanoic acid (*rac*-**3**) using

Reformatsky reaction.

Optical resolution of racemic 3-hydroxy-5-phenylpentanoic acid (*rac*-3) with cinchonidine:

The influence of solvents used for recrystallization on the optical resolution of *rac*-**3** with cinchonidine was investigated. The initial diastereomeric salt mixture was prepared by dissolving equimolar quantities of *rac*-**3** and cinchonidine in methanol followed by evaporation. It was then recrystallized from various solvents as described below. A small

quantity of the deposited salt was utilized to extract **3**; the recovered **3** was converted to methyl ester; its enantiopurity was determined by HPLC analysis (Table 1).

Table 1: Optical resolution of racemic 3-hydroxy-5-phenylpentanoic acid (*rac*-**3**) with cinchonidine[a]

Entry	Recrystallization solvent (mL)	Ratio of the salt to solvent included [b]	Yield % [c]	Ee % [d]	Eff. % [e]
1	50% EtOH (0.4)	Not included	87.0	62 (*R*)	54
2	EtOH (0.3)	Not crystallized	-	-	-
3	2-PrOH (0.3)	Not included	67.6	62 (*R*)	42
4	Toluene (0.5)	Not included	98.4	57 (*R*)	56
5	THF (0.7)	Not included	83.7	45 (*R*)	38
6	1,4-Dioxane (0.3)	Not included	98.6	55 (*R*)	54
7	$CHCl_3$ (0.3)	Not included	81.8	12 (*R*)	10
8	AcOEt (2.2)	Not included	97.9	47 (*R*)	46
9	Acetone (18.5)	Not included	30.8	81 (*R*)	25

a) 0.25 mmol *rac*-**3** and cinchonidine were used.
b) The solvent inclusion was evaluated by ^{1}H NMR analysis.
c) The yield is based on half the amount of salt.
d) The Ee was determined by HPLC after derivatization to its corresponding methyl ester.
e) Eff. (%) = Yield (%) × Ee (%) / 100.

The crystallization of the diastereomeric salts of *rac*-**3** and cinchonidine in 50% EtOH afforded the (*R*)-**3** salt with high resolution efficiency (entry 1). The diastereomeric salts of *rac*-**3** and cinchonidine did not crystallize in EtOH (entry 2), whereas 2-PrOH afforded the (*R*)-**3** salt with good efficiency (entry 3). Crystallization with toluene produced outstanding results and afforded the (*R*)-**3** salt in high enantiomeric excess as well as overall high efficiency (entry 4). Good resolution efficiencies were observed when THF and AcOEt were used as the crystallization solvents, which yielded the (*R*)-**3** salt (entries 5 and 8). When 1,4-Dioxane was used as the crystallization solvent, (*R*)-**3** salt was obtained with high efficiency similar to the case of 50% EtOH and toluene (entry 6). The resolution indicated that $CHCl_3$ produced (*R*)-**3** salt with very low resolution efficiency (entry 7). The enantiopurity increased significantly when acetone was used as the crystallization solvent, which afforded the (*R*)-**3** salt, but the resolution efficiency dropped to a moderate value (entry 9).

Based on the above results, the resolution of *rac*-**3** with cinchonidine afforded very good results than the resolution of *rac*-**3** with (−)-ADPE. Especially, highly efficient optical resolution was afforded by crystallization in toluene.

Crystallographic analysis of diastereomeric salt:

Crystallographic investigation was performed to elucidate the chiral recognition during the resolution of *rac*-**3** with cinchonidine.

The crystal structures of the less-soluble diastereomeric salt (*R*)-**3** · cinchonidine obtained in AcOEt were analyzed and compared with crystal structures of other cinchonidine salts[20] ((*R*)-**1** · cinchonidine and (*R*)-**2** · cinchonidine) to unravel the chiral recognition.

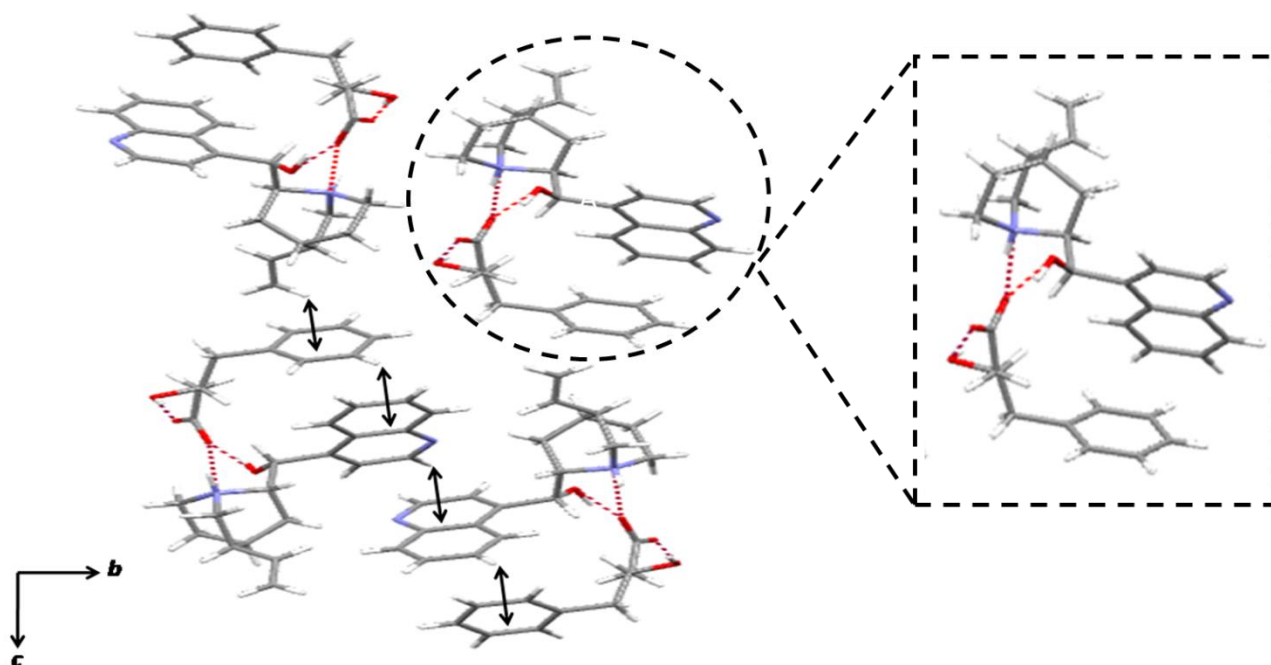**The less-soluble diastereomeric salt (*R*)-1 · cinchonidine obtained in EtOH[20]:**

Fig. 2. The (*R*)-**1** · cinchonidine salt obtained in an EtOH solution, viewed from the *a* axis. The dotted lines and arrows indicate hydrogen bonds and CH/π interactions, respectively.

The structure of the needle-like crystals (*R*)-**1** · cinchonidine obtained in EtOH is illustrated in Fig. 2. The ratio of **1** : cinchonidine was found to be 1:1. The absolute configuration of **1** was inferred to be (*R*), which was consistent with the resolution results. One carboxylate oxygen of (*R*)-**1**, which points towards the cinchonidine molecule, formed an intermolecular hydrogen bond with the ammonium hydrogen of the azabicyclo[2.2.2]octane group of cinchonidine. The same carboxylate oxygen was held by another intermolecular hydrogen bond that connected it to the hydroxy hydrogen of another cinchonidine. Another carboxylate oxygen of (*R*)-**1**, which points away from the cinchonidine molecule, was also involved in the intermolecular hydrogen bonding with the hydroxy hydrogen of other (*R*)-**1**. Thus, an array of structures with ribbon-like hydrogen-bonding patterns was present along the *a* axis. These hydrogen-bonding interactions are responsible for reinforcing crystal structure. The crystal structure was also reinforced by continuous CH/π interactions on the aromatic rings of **1** and cinchonidine. The phenyl group of (*R*)-**1** and the quinoline group of cinchonidine were arranged in an edge-to face orientation. One CH/π interaction was present between the CH of the quinoline group of cinchonidine and the quinoline group of other cinchonidine. Three CH/π interactions were present on the phenyl group of (*R*)-**1**, one is between the CH of the quinoline group of cinchonidine and the phenyl group of (*R*)-**1**, the other is between the *meta*-CH of (*R*)-**1** and the quinoline group of cinchonidine. Also, the CH of the vinyl group of cinchonidine was involved in the CH/π interaction with the phenyl group of (*R*)-**1**. These CH/π interactions were responsible for the recognition of benzyl group on the chiral center of (*R*)-**1**.

The less-soluble diastereomeric salt (*R*)-2 · cinchonidine obtained in EtOH/toluene[20]:

Fig. 3. The (*R*)-2 · cinchonidine salt obtained in an EtOH/toluene solution, viewed from the *a*

axis. The dotted lines and arrows indicate hydrogen bonds and CH/π interactions,

respectively.

The crystal structure of (*R*)-2 · cinchonidine salt, which was obtained in EtOH/toluene,

is shown in Fig. 3. The ratio of **2** : cinchonidine was found to be 1:1. The structure was

analogous to that of (*R*)-**1** · cinchonidine despite the presence of a chlorine substituent in **2**,

which explains the reason for high efficiency during the resolution of *rac*-**2**.

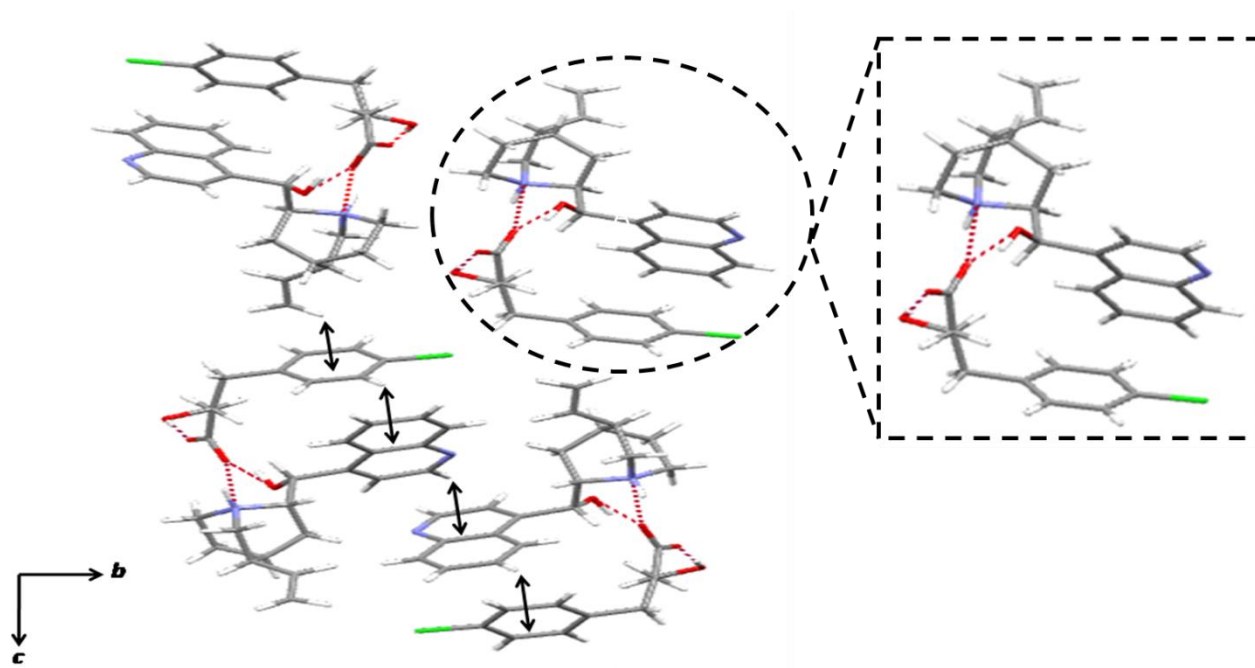**The less-soluble diastereomeric salt (*R*)-3 · cinchonidine obtained in AcOEt:**
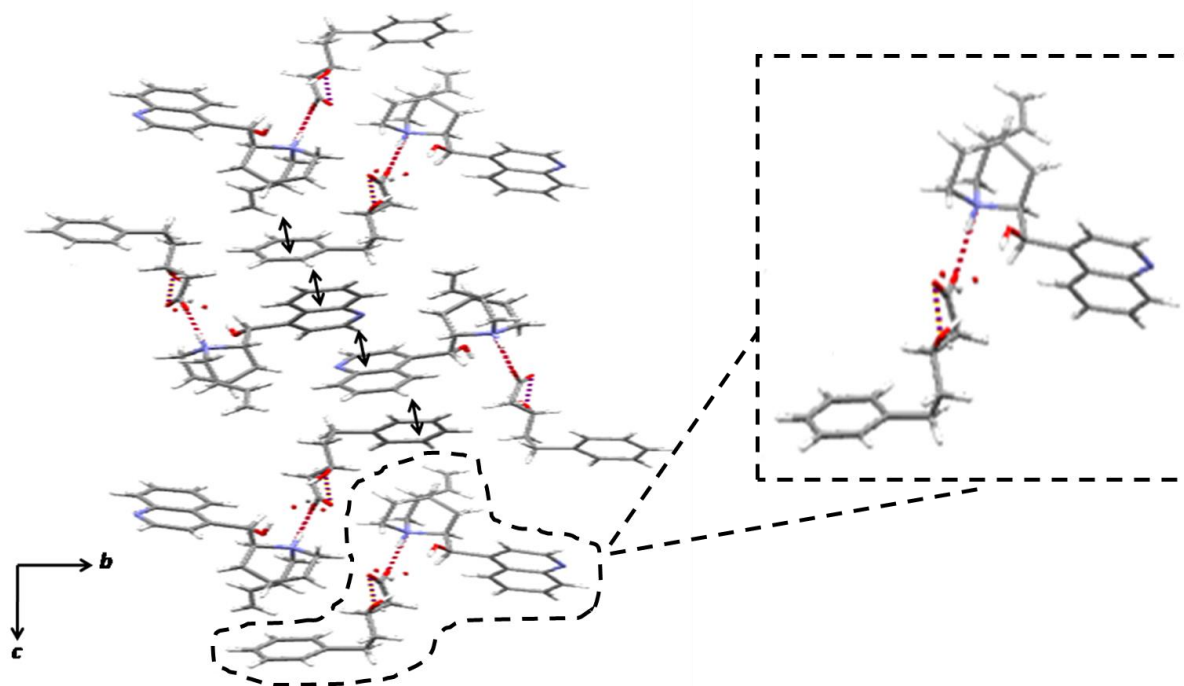

Fig. 4. The (*R*)-**3** · cinchonidine salt obtained in an AcOEt solution, viewed from the *a* axis. The dotted lines and arrows indicate hydrogen bonds and CH/π interactions, respectively.

The crystal structure of (*R*)-**3** · cinchonidine salt obtained using AcOEt is illustrated in Fig. 4. The ratio of **3** : cinchonidine was found to be 1:1. The absolute configuration of **3** was inferred to be (*R*), which was consistent with the resolution results (Table 1, entry 8). Although the carboxylate moiety of (*R*)-**3** was partly disordered, one carboxylate oxygen of (*R*)-**3**, which points towards the cinchonidine molecule, formed an intermolecular hydrogen bond with the ammonium hydrogen of the azabicyclo[2.2.2]octane group of cinchonidine. Another carboxylate oxygen of (*R*)-**3**, which points away from the cinchonidine molecule, was involved in the intramolecular hydrogen bonding with the hydroxy hydrogen of (*R*)-**3**. There are less intermolecular interactions in (*R*)-**3** · cinchonidine than in the (*R*)-**1** · cinchonidine salt, which probably contributed to its high solubility. They featured ribbon-like networks but only weakly

connected along the *a* axis. Also (*R*)-**3** · cinchonidine exhibited different packing patterns of arrays due to an additional methylene group. The phenyl group of (*R*)-**3** and the quinoline group of cinchonidine were positioned remote to each other. Nevertheless, the crystal structure was reinforced by the same type of continuous CH/π interactions as exhibited in (*R*)-**1** · cinchonidine and (*R*)-**2** · cinchonidine. Together with the fixation of carboxyl and hydroxy groups by hydrogen bonds, the terminal phenyl group of (*R*)-**3** was fixed with three kinds of CH/π interactions by cinchonidine. Despite its flexibility, *rac*-**3** was efficiently resolved using a large and rigid chiral structure, cinchonidine.

The probable reason that cinchonidine offered high resolution efficiency than ADPE during the resolution of *rac*-**3** would be attributed to the smaller structure of ADPE than cinchonidine, which was not suitable for chiral recognition of longer chain carboxylic acid, *rac*-**3**. On the other hand, cinchonidine is rigid and bulky and it can well distinguish (*R*) or (*S*) in the chiral center, although it is remote from the functional group, thereby contributing to high resolution efficiency. Moreover, there is no void space inside the crystal structure to allow the entry of solvent molecules and therefore solvent-induced chirality switching could not be applied to *rac*-**3**.

3.3 Conclusion:

The optical resolution of a 3-hydroxycarboxylic acid (with a more flexible substituent) *via* diastereomeric salt formation using cinchonidine was successfully demonstrated. The resolution of racemic 3-hydroxy-5-phenylpentanoic acid (*rac*-**3**) with cinchonidine afforded (*R*)-salt. In particular, highly efficient optical resolution was afforded by crystallization in toluene. Moreover, the resolution of *rac*-**3** with cinchonidine afforded very good results than the resolution of *rac*-**3** with (−)-ADPE. Crystallographic analysis revealed that hydrogen

bonding and CH/π interactions played a crucial role in chiral recognition by reinforcing the supramolecular structure of diastereomeric salt. This study guides the access of enantiomers with simple and economical operations. Further application of this unsophisticated method to other complex 3-hydroxycarboxylic acids is currently under investigation.

3.4 Experimental section:

3.4.1 General methods:

All the reagents and solvents were purchased and used as received. All ^{1}H NMR and ^{13}C NMR spectra were recorded on Bruker AVANCE 300, 400 or 500 MHz spectrometer. IR spectra were measured on a JASCO FT/IR-4600 spectrometer. Melting point was recorded on a MEL-TEMP apparatus and reported uncorrected. The enantiomeric excess values were determined by chiral HPLC analyses (Daicel Chiralcel OD-3 column; Eluent: 10% 2-PrOH in hexane; Flow rate: 1.0 mL/min).

3.4.2 Synthesis of 3-hydroxycarboxylic acid:

Synthesis of 3-hydroxy-5-phenylpentanoic acid ethyl ester: The *rac*-**3** ethyl ester has been synthesized using Reformatsky reaction. To a vigorously stirred mixture of activated zinc powder (1.04 g, 15.9 mmol) in dry THF (3 mL), ethyl bromoacetate (2.15 g, 12.9 mmol) diluted with dry THF (1.5 mL) was added dropwise slowly at room temperature. After 15 minutes, it was followed by the addition of 3-phenylpropanal (1.74 g, 13.0 mmol) diluted with dry THF (1.5 mL), dropwise slowly at room temperature. The reaction mixture was refluxed at 70 °C for 74 h under a N$_2$ atmosphere. During refluxing, dry THF (6 mL) was added. The reaction mixture was then ice cooled at 0 °C and acidified with 4N aqueous HCl (pH ~ 3). After removal of the volatiles, it was extracted with CHCl$_3$ (25 mL X 2). The combined organic layers were

washed with brine (25 mL), dried over anhydrous Na_2SO_4 and evaporated under vacuum. Finally the crude product was purified by silica gel column chromatography (eluent; hexane : ethyl acetate = 5 : 1) and obtained as pale yellow viscous liquid (1.48 g, 6.66 mmol). The yield was calculated to be 51.7 %. ^{1}H NMR (300 MHz, CDCl$_3$): δ (ppm) 7.35-7.14 (m, 5H), 4.16 (q, J = 7.2 Hz, 2H), 4.09-3.99 (m, 1H), 3.13-3.04 (m, 1H), 2.89-2.63 (m, 2H), 2.58-2.39 (m, 2H), 2.00-1.65 (m, 2H), 1.27 (t, J = 7.2 Hz, 3H). ^{13}C NMR (125 MHz, CDCl$_3$): δ (ppm) 173.0, 141.8, 128.5, 128.4, 125.9, 67.2, 60.7, 41.3, 38.1, 31.8, 14.2. IR (neat): ν(cm^{-1}) 3450, 3027, 2931, 1732, 1496, 1373, 1303, 1185, 1092, 1029, 700.

Synthesis of 3-hydroxy-5-phenylpentanoic acid (*rac*-3): To a stirred solution of 3-hydroxy-5-phenylpentanoic acid ethyl ester (1.48 g, 6.66 mmol) in MeOH (45 mL), 2M aqueous KOH (7.5 mL) was added dropwise at 0 °C. The reaction mixture was stirred at room temperature for 62 h. It was ice cooled at 0 °C and acidified with 6N aqueous HCl (pH ~ 3) and extracted with chloroform (30 mL X 3). The combined organic layers were washed with brine (30 mL), dried over anhydrous Na_2SO_4 and evaporated under vacuum. Finally, the crude product was recrystallized from CHCl$_3$ and *rac*-3 was obtained as a white solid (1.05 g, 5.41 mmol). The yield was calculated to be 81.2%. Mp. 133-135 °C. ^{1}H NMR (300 MHz, CD$_3$OD): δ (ppm) 7.29-7.11 (m, 5H), 4.03-3.94 (m, 1H), 2.84-2.59 (m, 2H), 2.51-2.31 (m, 2H), 1.87-1.66 (m, 2H). ^{13}C NMR (125 MHz, CD$_3$OD): δ (ppm) 175.5, 143.4, 129.5, 129.4, 126.8, 68.7, 43.3, 40.1, 32.9. IR (KBr): ν(cm^{-1}) 3222, 3028, 2924, 1683, 1494, 1455, 1354, 1304, 1273, 1090, 934, 706.

3.4.3 Optical resolution of *rac*-3 with cinchonidine:

The resolution experiment was carried out as follows: Equimolar amounts of *rac*-**3** and cinchonidine were dissolved in methanol followed by evaporation under vacuum. After concentration, the resulting white solid was recrystallized from a suitable solvent. The obtained crystals were filtered; dried overnight. The apparent yield was calculated based on half the amount of salt. A small portion of the salt was decomposed by the addition of 1N aqueous HCl solution and extracted with diethyl ether. The organic phase was collected and washed with water. Further it was dried over anhydrous Na_2SO_4 and concentrated to obtain **3**. After derivatizing **3** to its corresponding methyl ester by employing $TMSCHN_2$, chiral HPLC analysis was performed.

3 methyl ester: (Daicel Chiralcel OD-3 column; Eluent: 10% 2-PrOH in hexane; Flow rate: 1.0 mL/min) $t_r(S)$ = 12.0 min, $t_r(R)$ = 13.8 min.

3.4.4 Single crystal X-ray analysis of the diastereomeric salt crystals:

Single crystals suitable for X-ray diffraction analysis were prepared by slow evaporation of the saturated solutions of the diastereomeric salt. X-ray crystallographic data were collected on a Bruker Smart APEX II diffractometer with graphite monochromated Mo-Kα radiation. Crystal data for (*R*)-**1** · cinchonidine: $C_{29}H_{34}N_2O_4$, M = 474.58, orthorhombic, *a* = 6.2815(10), *b* = 15.074(2), *c* = 26.456(4) Å, *V* = 2505.1(7) Å^3, *T* = 150 K, space group $P2_12_12_1$, *Z* = 4, 12041 reflections measured, 4410 independent reflections, The final R_1 was 0.0496 (I > 2σ(I)) and $wR(F_2)$ was 0.1237 (I > 2σ(I)), CCDC: 2173287. Crystal data for (*R*)-**2** · cinchonidine: $C_{29}H_{33}N_2O_4Cl$, M = 509.02, orthorhombic, *a* = 6.308(4), *b* = 15.189(9), *c* = 26.885(16) Å, *V* = 2576(3) Å^3, *T* = 150 K, space group $P2_12_12_1$, *Z* = 4, 12137 reflections measured, 4544

independent reflections, The final R_1 was 0.0528 (I > 2σ(I)) and wR(F$_2$) was 0.1211 (I > 2σ(I)),

CCDC: 2173288. Crystal data for (*R*)-**3** · cinchonidine: $C_{30}H_{36}N_2O_4$, M = 488.61, orthorhombic,

a = 6.4241(12), *b* = 15.084(3), *c* = 26.364(5) Å, *V* = 2554.8(8) Å^3, *T* = 150 K, space group $P2_12_12_1$,

Z = 4, 15052 reflections measured, 5841 independent reflections, The final R_1 was 0.091 (I >

2σ(I)) and wR(F$_2$) was 0.2461 (I > 2σ(I)), CCDC: 2173289.

3.5 References:

1. Thaisrivongs, S.; Pals, D. T.; Kati, W. M.; Turner, S. R.; Thomasco, L. M.; Watt, W. *J. Med. Chem*. **1986**, *29*, 2080.

2. Schostarez, H. J. *J. Org. Chem*. **1988**, *53*, 3628.

3. Oertle, K.; Beyeler, H.; Duthaler, R. O.; Lottenbach, W.; Riediker, M.; Steiner, E. *Helv. Chim. Acta* **1990**, *73*, 353.

4. Seidel, W.; Seebach, D. *Tetrahedron Lett.* **1982**, *23*, 159-162.

5. Masamune, S.; Choy, W.; Petersen, J. S.; Sita, L. R. *Angew. Chem., Int. Ed. Engl.* **1985**, *24*, 1.

6. Nicolaou, K. C.; Chakraborty, T. K.; Ogawa, Y.; Daines, R. A.; Simpkins, N. S.; Furst, G. T. *J. Am. Chem. Soc*. **1988**, *110*, 4660.

7. Tatsuta, K.; Amemiya, Y.; Kanemura, Y.; Takahashi, H.; Kinoshita, M. *Tetrahedron Lett.* **1982**, *23*, 3375.

8. Schlessinger, R. H.; Poss, M. A.; Richardson, S. *J. Am. Chem. Soc.* **1986**, *108*, 3112.

9. Sandoval, A.; Arias-Barrau, E.; Bermejo, F.; Canedo, L.; Naharro, G.; Olivera, E.; Luengo, J. *Appl. Microbiol. Biotechnol.* **2005**, *67*, 97-105.

10. Burke, T. R.; Knight, M.; Chandrasekhar, B. *Tetrahedron Lett.* **1989**, *30*, 519-522.

11. Takashi, M.; Isao, T.; Kenji, F. *Bull. Chem. Soc. Jpn.* **1971**, *44*, 3378.

12. Olma, A. *Polish J. Chem.* **1996**, *70*, 1442.

13. Madsen, U.; Frydenvang, K.; Ebert, B.; Johansen, T. N.; Brehm, L.; Krogsgaard-Larsen, P. *J. Med. Chem.* **1996**, *39*, 183-190.

14. Kodama, K.; Shitara, H.; Hirose, T. *Cryst. Growth Des.* **2014**, *14*, 3549-3556.

15. Kodama, K.; Kawasaki, K.; Yi, M.; Tsukamoto, K.; Shitara, H.; Hirose, T. *Cryst. Growth Des.* **2019**, *19*, 7153-7159.

16. Kodama, K.; Yi, M.; Shitara, H.; Hirose, T. *Tetrahedron Lett.* **2020**, *61*, 151773.

17. Kodama, K.; Kurozumi, N.; Shitara, H.; Hirose, T. *Tetrahedron* **2014**, *70*, 7923–7928.

18. Chandrasekaran, S.; Hirose, T.; Kodama, K. *Tetrahedron* **2022**, *108*, 132653.

19. Kodama, K.; Nagata, J.; Kurozumi, N.; Shitara, H.; Hirose, T. *Tetrahedron: Asymmetry* **2017**, *28*, 460-466.

20. Tambo, M. *Master's thesis,* Saitama University, **2021**.

21. Suezawa, H.; Ishihara, S.; Umezawa, Y.; Tsuboyama, S.; Nishio, M. *Eur. J. Org. Chem.* **2004**, *2004*, 4816–4822.

22. Yoji, U.; Sei, T.; Kazumasa, H.; Jun, U.; Motohiro, N. *Bull. Chem. Soc. Jpn.* **1998**, *71*, 1207–1213.

CHAPTER 4

Conclusion and Outlook

This chapter summarizes my research work.

In **chapter 2**, solvent-induced chirality switching, in the optical resolution of chlorine-substituted TAs with (−)-ADPE has been demonstrated. In the case of 2-Cl-TA, resolution in branched alcohols such as *i*-PrOH and *s*-BuOH afforded (*R*)-2-Cl-TA · (−)-ADPE as a less-soluble diastereomeric salt, whereas the (*S*)-2-Cl-TA · (−)-ADPE salt was obtained in linear alcohols such as MeOH, EtOH, and *n*-PrOH. The stereoselectivity was switched by employing different types of solvents. The crystal structures revealed that the incorporation of solvent into the (*S*)-2-Cl-TA salt contributed to its stability. On the other hand, solvent-induced chirality switching could not be achieved with 3-Cl-TA and 4-Cl-TA. The structural effect associated with changing the position of the chlorine substituent from the *ortho* to the *meta* or *para* position on solvent-induced chirality switching was also discussed.

This study has expanded the scope of the solvent-induced chirality switching resolution to a halogen-substituted derivative of TA and will provide an unsophisticated technique for accessing both enantiomers of 2-F-TA, and 2-Br-TA without changing the resolving agent. The crystallographic discussion will provide a deep insight for designing metal organic frameworks and inclusion crystals for various applications such as sensing, catalysis, separation, purification and energy storage. These findings will be also useful in designing novel drug delivery systems and supercapacitors.

In **chapter 3**, the optical resolution of a 3-hydroxycarboxylic acid with a more flexible substituent *via* diastereomeric salt formation using cinchonidine was successfully demonstrated. The resolution of racemic 3-hydroxy-5-phenylpentanoic acid (*rac*-**3**) with cinchonidine afforded (*R*)-salt. In particular, highly efficient optical resolution was afforded by crystallization in toluene. Moreover, the resolution of *rac*-**3** with cinchonidine afforded very good results than the resolution of *rac*-**3** with (−)-ADPE. Crystallographic analysis revealed that hydrogen bonding and CH/π interactions played a crucial role in chiral recognition by reinforcing the supramolecular structure of diastereomeric salt.

Herein, we have expanded the scope of the optical resolution *via* diastereomeric salt formation to a 3-hydroxycarboxylic acid with a more flexible substituent, which will provide a guiding concept for us to access enantiomers with simple and economical operations. This method could be further applied to other 3-hydroxycarboxylic acids with a more flexible substituent like 3-hydroxy-6-phenylhexanoic acid, 3-hydroxy-7-phenylheptanoic acid, *etc*,. The results of the crystallographic investigation will help us to understand the 3D structures and properties of various complex biomolecules such as proteins and nucleic acids. These findings will also help us to understand the molecular interactions such as protein-protein interactions in tissue engineering.

Publications and Presentations

List of publications

Chapter 2

"*Solvent-induced chirality switching*" in the enantioseparation of chlorine-substituted tropic acids via diastereomeric salt formation by (1*R*,2*S*)-(−)-2-amino-1,2-diphenylethanol (ADPE). <u>Srinivas Chandrasekaran</u>, Takuji Hirose and Koichi Kodama, *Tetrahedron*, **2022**, *108*, 132653.

Chapter 3

Enantioseparation of 3-hydroxycarboxylic acids via diastereomeric salt formation by 2-amino-1,2-diphenylethanol (ADPE) and cinchonidine. <u>Srinivas Chandrasekaran</u>, Masaki Tambo, Yuta Yamazaki, Tatsuro Muramatsu, Yusuke Kanda, Takuji Hirose and Koichi Kodama, *Molecules,* **2023**, *28(1),* 114.

Related Publication List

Co/Co-N@Nanoporous Carbon Derived from ZIF-67: A Highly Sensitive and Selective Electrochemical Dopamine Sensor. <u>Chandrasekaran Srinivas</u>, Murugesan Sudharsan, G. Rajendra Kumar Reddy, P. Suresh Kumar, Arlin Jose Amali and D. Suresh, *Electroanalysis,* **2018**, *30*, 2475 − 2482.

Presentations at conferences

1. Solvent-induced chirality switching effect in the enantioseparation of 2-chlorotropic acid by (1*R*,2*S*)-(−)-2-amino-1,2-diphenylethanol. <u>Srinivas Chandrasekaran</u>, Takuji Hirose and Koichi Kodama, The 101st CSJ Annual Meeting, March 20, 2021.

2. "*Solvent-Induced Chirality Switching*" in the enantioseparation of chlorine-substituted tropic Acids via diastereomeric salt formation. <u>Srinivas Chandrasekaran</u>, Takuji Hirose and Koichi Kodama, Symposium on Molecular Chirality, November 30, 2021.

3. "*Solvent-Induced Chirality Switching*" in the enantioseparation of chlorine-substituted tropic Acids via diastereomeric salt formation. <u>Srinivas Chandrasekaran</u>, Takuji Hirose and Koichi Kodama, The 102nd CSJ Annual Meeting, March 26, 2022.

Acknowledgements

Firstly, I express my deep gratitude to my supervisor, **Prof. Dr. Koichi Kodama**, Saitama University, for his patience, motivation, and immense knowledge that helped me to achieve a successful research activity in my Ph. D. His guidance helped me in all the time of research and writing of research papers. I thank him for being a good support to me along with being an advisor and mentor for my Ph. D. study. I strongly believe that I have gained a lot of knowledge and skills during my Ph. D. from his esteemed supervision.

I would like to express my sincere gratitude and gratefulness to **Prof. Dr. Takuji Hirose**, Saitama University, for giving me the opportunity to join his research team for my Ph. D. His continuous support, guidance, and suggestions for my research and for the financial support through MEXT scholarship have helped me to pursue my Ph. D. smoothly.

I would like to express my sincere thanks to my co-advisors, **Prof. Dr. Masuki Kawamoto,** RIKEN; **Prof. Dr. Takashi Fujihara** and **Prof. Dr. Koji Matsuoka**, Saitama University, for their continuous support during my Ph. D. study. Their supervision and suggestions related to my research helped me to have a smooth and successful progress in my research. I sincerely appreciate their support, valuable time, and endless efforts since my admission until my graduation.

My sincere thanks to **Dr. Hiroaki Shitara** and **Dr. Mikio Yasutake** for supporting my research activities.

My special thanks to all my friends in organic industrial chemistry laboratory for their kind help, motivation and encouragement during my research activities as well as my stay in Japan.

My heartful thanks to my dear parents, wife and my family members for their constant support and encouragement that made me stronger to overcome tough situations and ease my stay in Japan until my graduation.

Last but not the least, I would like to praise and thank God, the Almighty, who has granted countless blessing, knowledge, opportunity, and support to grow as a better person.